This is a peer-reviewed, author's accepted manuscript of the following research article: Abdulhussein Al-Ali, A. A., Al Ward, N., Obeid, M. A., Nielsen, C. U., Mulheran, P. A., & Al Qaraghuli, M. M. (Accepted/In press). Recent advances in photothermal therapies against cancer and the role of membrane transporter modulators on the efficacy of this approach. *Technology in Cancer Research & Treatment*. https://doi.org/10.1177/15330338231168016

Title:

Recent advances in photothermal therapies against cancer and the role of membrane transporter modulators on the efficacy of this approach.

Authors:

Ahmed A. Abdulhussein Al-Ali[1,2], Nameer Al Ward[3], Mohammad A. Obeid[4,5], Carsten Uhd Nielsen[1], Paul A. Mulheran[6], Mohammed M. Al Qaraghuli[4,7,8*]

Affiliations:

[1]Department of Physics, Chemistry and Pharmacy, University of Southern Denmark, Campusvej 55, 5230 Odense M, Denmark.

[2]Basra University College of Science and Technology, Al-Wofod street, Basra, Iraq.

[3]Sultan Qaboos Comprehensive Cancer Care & Research Centre, Muscat, Sultanate of Oman.

[4]Strathclyde Institute of Pharmacy and Biomedical Sciences, University of Strathclyde, 161 Cathedral Street, Glasgow, UK

[5]Department of Pharmaceutics and pharmaceutical technology, Faculty of Pharmacy, Yarmouk University, Irbid, Jordan.

[6]Department of Chemical and Process Engineering, University of Strathclyde, 75 Montrose Street, Glasgow, G1 1XJ, UK

[7]EPSRC Future Manufacturing Research Hub for Continuous Manufacturing and Advanced Crystallisation (CMAC), University of Strathclyde, 99 George Street, Glasgow, G1 1RD, UK

[8]SiMologics Ltd., Glasgow, UK

* Corresponding author. Email address: m.alqaraghuli@simologics.co.uk

Keywords

Photothermal therapy, gold nanoparticles, monoclonal antibodies, and membrane transporters.

Abstract:

Recently, much research is focused on the use of Photothermal therapy (PTT) as an advanced method to treat various types of cancer. The PTT approach primarily utilises nanoparticles (NPs) made from metals, carbon or semiconductors that can convert near-infrared laser irradiation, which penetrates tissues, into local heat that induces cancer cell death. An alternative approach is to utilise NPs (such as liposomes) to carry suitable dye molecules to the same end. Numerous studies concerning PTT have shown that local heat released in cancer cells may suppress the expression of membrane transporter proteins such as P-glycoprotein (P-gp) and multidrug resistance-associated protein 1 (MRP1), thus enhancing cytotoxicity and reverse multidrug resistance. In addition, because NPs may be loaded with different substances, researchers have designed multifunctional NPs for PTT by including several agents such as membrane transporter modulators, anticancer drugs, and photothermal agent. This review will focus on the recent advances in PTT utilising various types of NPs, and their components and characteristics. In addition, the role of membrane transporters in PTT will be highlighted and different methods of transporter modulation will be summarised from several PTT studies in which multifunctional NPs were used to treat cancers *in vitro* and *in vivo*.

Introduction:

Cancer is a group of diseases that affects millions of patients annually. According to the World Health Organisation (WHO), cancer accounted for nearly 10 million deaths in 2020; and the most common types of cancer affected the breast, lung, colon, prostate, skin, and stomach [1]. For instance, in 2022, 1,918,030 new cancer cases were projected to occur in the United States [2], and around 3 million people are currently living with cancer in the UK [3]. These horrible numbers could adversely progress due to the Coronavirus disease 2019 (COVID-19) pandemic that led to delays in both diagnosis and treatment [4].

The main cancer treatment modalities are surgery, radiotherapy (RT), chemotherapy (CT), and biotherapeutic antibodies. However, these therapies could be either associated with severe side effects or not being sufficiently effective [5,6]. The recent technological advances have enhanced our understanding of cancer and the importance of using multi-disciplinary approach to tackle this disease. Photothermal therapy (PTT) is an approach that has attracted extensive research attention as a non-invasive and selective treatment strategy for numerous cancers [7]. The photothermal concept depends on photothermal agents that convert light (typically near-infrared) energy into heat, thus increasing the temperature of surrounding tissue and triggering cancer cell death [8]. These agents typically possess the ability for specific targeting and high photothermal conversion efficiency without excessive thermal damage to surrounding tissues [9].

Various review articles have focused on different aspects of the PTT including properties of the implemented nanoparticles, temperature optimisation, and their clinical development [10–12]. In addition, several articles showed that the heat generated from PTT may enhance the cytotoxicity of PTT in cancer cells [13–15]. This enhancement

was related to the effect of heat on the expression of membrane transporters which is one of the major causes of the multidrug resistance phenomenon. Much research thereafter has shown that loading of PTT nanoparticles with membrane transporter modulators improved the outcomes of PTT both *in vitro* and *in vivo* [16–18]. Consequently, this review will specifically provide an updated summary on the current advances in this field and will highlight the important role of membrane transporters on the efficacy of the PTT approach.

The nanoparticle component of PTT:

Nanotechnology has rapidly evolved over the past few years to provide significant potential in combating cancer [19]. Nanoparticles exhibit unique characteristics that enhance their application in the field of cancer treatment. These mainly include their selective accumulation into tumour tissues, their versatile structures which facilitate their surface modification for enhanced targeting, along with their ability to load various types of therapeutic agents [20]. The large surface to volume ratio of nanoparticles represents additional advantage [21]; the nanoparticle surfaces can be densely coated with different molecules that have targeting properties [22] as well as other functionalities.

In order to meet the high nutrient and oxygen demands, tumour tissues are characterised by massive and irregular neovascularization in with structural and functional abnormalities in the blood vessels presented as very dense and tortuous with fenestrated structure. This will facilitate the penetration of macromolecular compounds with sizes above 40 kDa [23,24]. Moreover, these tissues do not have efficient lymphatic drainage system which will result in the trapping of the penetrated macromolecules inside the tumour tissues for prolonged period of time [25,26]. Together,

the increase in the penetration of macromolecules and their retention in the tumour tissues, form the enhanced permeability and retention phenomena (EPR). The EPR phenomena has been observed in various solid tumours in rodents, rabbits, dogs, and humans [27–29]. This effect has been later used in the targeting of the anticancer therapeutics into the solid tumour by controlling the size and the characteristics of the drug delivery system [30]. Nanoparticles can be effectively used for this purpose since they can accumulate in cancer tissues due to the EPR effects [31]. Different factors seems to affect the use of nanoparticles in PTT including their size, surface properties, shape, and concentration [32].

The ability of gold nanoparticles to absorb light in the visible as well as the near infrared (NIR) region depends on the gold nanoparticle shape and dimension, which influences the surface plasmon resonance (SPR) required for the photothermal effect. Depending on the dimensions, gold nanoparticles can be classified into three categories. One dimensional gold nanoparticles include gold nanobelts, nanowires, nanotubes, and gold nanorods. Two-dimensional gold nanoparticles include dimpled gold nanoparticles, truncated triangles, square or rectangular nanoparticles, and hexagonal nanoparticles. All these two-dimensional gold nanoparticles are referred to as gold nanoplates. Three-dimensional gold nanoparticles include the nanodumbbells, nanotadpoles, nanostars, nanodendrites, and nanopods. The last three types are considered as branched gold nanoparticles [33].

These different types of gold nanoparticle have various characteristics and applications. They differ from each other in terms of their physicochemical characteristics, SPR, optical and electronic properties [34,35]. These differences resulted from the variability of the size, shape, and aspect ratio. The availability of different types of gold nanoparticles which can be easily synthesised has resulted in various

applications in many fields such as diagnosis and imaging, targeted drug delivery into specific diseased tissue or organ, biosensing, and most importantly in photothermal and photodynamic therapy [36].

A wide range of nanoparticles have been adopted in PTT-based cancer treatments, such as metal nanomaterials (platinum and gold), carbon nanomaterials (graphene and carbon nanotubes), semiconductor nanomaterials (copper), and conducting polymers [37,38]. By changing the size and shape of AuNPs, the SPR can be tuned to the NIR region, which imparts high depth photothermal penetration in tissues [39].

Semiconducting polymer-based nanoparticles (SPNs) used for PTT exhibit favourable properties such as biological compatibility and excellent optical properties. Li et al. synthesised highly biodegradable SPNs with photothermic activity which upon NIR irradiation resulting in a local temperature increase up to 45 °C leading to collagen digestion in the tumour extracellular matrix [40].

Metal based nanoparticles, especially gold nanoparticles, exhibit excellent photothermal activities due to their abilities to passively accumulate in the tumour tissues by the EPR effect and their strong absorbance of NIR light. The NIR exposure of these nanoparticles will enhance the resonance of the high number of free electrons presented within the metal and on its surface and induce SPR. This will result in high photothermal conversion activity which will promote apoptosis and necrosis in the cancerous tissues. Once accumulated at the tumour tissues, gold nanoparticles can strongly absorb the irradiated laser alight and immediately generate heat locally with minimal damage to the adjacent normal tissues.

Iron oxide nanoparticles (IONPs) are another metal-based nanoparticle with magnetic properties. They are safe, biocompatible, with high ability to absorb both visible and NIR light and generate heat for PTT [41]. Similar to other nanoparticles, IONPs can

accumulate in the tumour tissues based on the EPR effect and the generated heat from the IONPs can result in an intense cancer cell death. Moreover, since these nanoparticles have magnetic properties, their accumulation in the cancer tissues can be increased by applying an external magnetic field before exposing them to NIR light. This external magnetic field can also result in the generation of magnetic hyperthermia with a subsequent destruction to cancer cells [42]. Moreover, the iron presented in these nanoparticles can contribute to the iron haemostasis in the body after the metabolism of these IONPs into elemental iron.

Quantum dots (QD) contain several types of materials and are characterised by their small size which promote their use in PTT. The optical properties of QD can be adjusted by controlling their size and composition which can result in improved heat generation, high production of reactive oxygen species (ROS), and fast metabolic rate to avoid long exposure toxicity. Black phosphorus quantum dots (BPQDs) are one type of QD that exhibit novel PTT. BPQDs with a lateral size around 2.6 nm have efficient NIR photothermal performance with high photostability. Under irradiation with 808 nm laser, BPQDs resulted in complete *in vitro* killing of cancer cells. Moreover, in the absence of irradiation, these types of nanoparticles have negligible toxicity even at high concentrations resulting in high biocompatibility profile [43].

Carbon nanotubes are a class of carbon-based nanoparticles that are employed in PTT based on their ability to absorb light energy at wavelengths from 750-1000 nm followed by heat generation. Carbon nanotubes are present as either single walled carbon nanotubes (SWCNTs) or multiple walled carbon nanotubes (MWCNTs) based on the number of the tube wall layers. The SWCNTs developed by Liang et al. exhibited an effective destruction of metastatic tumours in an *in vivo* mice model. This was a result of the accumulation of these SWCNTs in the tumour followed by heat

generation in response to light irradiation [44]. Yang et al. developed PEGylated nanographene sheets (NGS) coated with polyethylene glycol with a size of 10–50 nm in the form of 1–2 layers which showed high tumour accumulation through passive targeting. These NGS showed strong optical absorbance in the NIR region which resulted in a temperature increase by more than 30 °C with a subsequent efficient tumour ablation based on this PTT [45].

MnO_2 nanosheets have been also applied in the field of PTT. pH-/H_2O_2-responsive MnO_2 nanosheets anchored with up-conversion nanoprobes were developed by Fan et al. These can exert excellent PTT under hypoxic conditions by the conversion of the NIR into short wavelength light which will result in a local temperature increase. In this system, the pH and the H_2O_2 consumption at tumour sites will result in oxygen production to enhance the PTT and at the same time the emitted light quenching of in this system protects the normal tissues from ROS-mediated damage [46].

For more efficient cancer treatment, several types of the nanoparticles used to exert PTT can also be loaded with some chemotherapeutic anticancer agents to achieve enhanced synergistic effect between the chemotherapy and the PTT. In this regard, the nanoparticle will act as a carrier to deliver the loaded drug into the target cancer cells based on the EPR effect and the same nanocarrier will absorbed the NIR light to induce PTT. This will improve the therapeutic outcomes of chemotherapy when combined with PTT using the same nanocarrier. This can be seen in the work of Wu et al. who developed an engineered versatile nanoplatform based on graphene oxide (GO) coated with mesoporous silica for synergetic effect between the PTT and doxorubicin. The GO is used for improved photothermal effects, and the mesoporous silica will enhance the doxorubicin loading. The *in vivo* study demonstrated that these nanoplatform could accumulate in the cancer cells by the EPR effect and the NIR can

trigger doxorubicin release and result in a local temperature increase to above 50 °C exhibiting excellent antitumour synergy between chemotherapy and PTT [47]. Other platforms have employed Cisplatin as a loading agent. Similar to Doxorubicin, Cisplatin have showed enhanced localised antitumour effects by improving hypoxia at the site of action [48].

Liposomes, which are the mostly studied type of nanoparticles, are also investigated in PTT. Liposomes are composed of phospholipids, cholesterol, and other components which will self-assemble into a bilayer structure upon hydration [49]. Liposomes components by themselves have poor light absorption properties, however, their use in PTT is based on loading NIR absorbing dyes, such as indocyanine green (ICG), IR780, IR820, and IR792. Following the accumulation of these loaded liposomes into the target cancers, the dyes will be released and used for PTT [50]. The used irradiation wavelength will depend on the selected dye loaded into the liposomes. Moreover, liposomes have another advantage in the context of PTT in that additional molecules can be co-loaded into liposomes such as chemotherapeutic agents for a synergetic effect between PTT and chemotherapy.

Xu et al. developed ICG-loaded liposomes wrapped with C6 glioma cell membranes for potential application in PTT. The liposomes enhanced the accumulation of the ICG dye in glioma tumours in BALB/c nude mice which showed a peak absorption at 808 nm resulting in complete tumour eradication within 18 days [51].

Other types of nanoparticles that can also be used in PTT include sulfide nanoparticles, silver nanoparticles, silica nanoparticles, palladium, and polymeric nanoparticles. Each one of them have different features and specific applications in the field of PTT with highly promising future outcomes.

Laser wavelength is also crucial in determining the outcomes of the AuNPs action, in majority of the AuNPs studied, 808 nm PTT laser wavelength was used. Few studies have employed other wavelengths, such as, 650nm, 980nm and 1064nm. However, the use of 808nm has proven to be the most efficient when it comes to most optimum temperature enhancements they cause compared to other wavelengths [52]. NIR irradiation with wavelengths between 650 and 1350 nm can be used for the excitation of some types of nanoparticles where the absorbed light can be converted to heat through plasmonic heating or nonradiative relaxation. This has led to an extensive investigation for the use of various types of nanoparticles in PTT either alone or in combination with other therapeutic agents.

The targeting component of PTT:

The excellent properties of nanoparticles can be improved through the conjugation of targeting molecules, such as monoclonal antibodies (mAbs), onto the surfaces of nanoparticles to enhance the targeting effect to certain cancer cells [53]. Antibodies are widely used in cancer due to their versatile targeting capability [54]. In addition, antibodies can directly target cancer cells while concurrently promoting the induction of long-lasting anti-cancer immune responses [55]. For example, antibodies could target tumour antigens, tumour microenvironment to reduce tumour growth, or to target cells of the immune system to enhance the anti-tumour immune responses [54]. In addition, antibodies could manipulate the host immune response to tumours through either Antibody-dependent cellular cytotoxicity (ADCC), complement-dependent cytotoxicity (CDC), or the induction of adaptive immune responses [9,56].

The microenvironment of cancer comprises several factors that can inhibit the immune responses against cancer, promote cancer cell growth, and induce pro-tumorigenic angiogenesis [57]. Targeting these critical factors and proteins within the cancer microenvironment was proven clinically through the successful approval of several antibodies against different forms of cancer. Consequently, mAbs represent major tools to fulfil this requirement.

Several articles highlighted the utilisation of AuNPs-mAbs conjugates within various photothermal approaches (Table 1). Different shapes of AuNPs were used, including nanorods (AuNR), nanoshells (AuNSH), nanostars (AuNST), and nanocages (AuNC). The high representation of AuNR could be attributed to their excellent physical properties represented by strong NIR absorption due to the longitudinal localised SPR band [58].

The mAbs that have shown promising efficacy (summarised in Table 1) include anti-HSP mAb used to target HSP70 expression in 4T1 cell lines [59]. In addition, an anti-HER2 mAbs were tested on SKBR3, MDA-MB-231, MCF-7 and CIK cells, and C57BL/6 and MCF-7 tumour bearing mice [60]. Another mAb that provided significant results is the anti-CD33 antibody that was conjugated with AuNST [61].

Different researchers have also investigated the coating of these AuNPs with other molecules like bovine serum albumin, polylactic-co-glycolic acid (PLGA), chitosan, and indocyanine green (ICG) to increase the stability of the AuNPs [62–64]. The implemented antibodies have mainly targeted Epidermal Growth Factor Receptors (EGFR) in multiple cancer cell lines since EGFR is the most commonly overexpressed membranous oncogenic protein in cancer [65]. Numerous cell lines were used to test these particles as for example in glioblastoma (U373-MG and 1321N1 cell lines)[66],

breast cancer (MDA-MB-231 and HeLa cells) [67], lung cancer (A549 cells) [68], and oral cancers (HOC313 clone 8 and HSC 3) [8].

Table 1: Summary of targeted therapy utilisation in gold nanoparticles

AuNC (gold nanocage), AuNR (gold nanorod), AuNSH (gold nano shell), AuNST (gold nano star), BSA (bovine serum albumin), PLGA (polylactic-co-glycolic acid), ICG (indocyanine green), HSP (heat shock proteins), EGFR (epidermal growth factor receptor), HER2 (human epidermal growth factor receptor 2), R837 (imiquimod), CD33 (transmembrane receptor), HSP70 (family of conserved ubiquitously expressed heat shock proteins), CD44 (cell-surface glycoprotein antigen), DCs (antigen-presenting cells for activating native T cells), CD8 (transmembrane glycoprotein), CD133 (prominin-1), PTT (photothermal therapy), 4T1 (Cell line posing 6-thioguanine resistance), U373-MG (human glioblastoma cell line), 1321N1 (human astrocytoma cell line), MDA-MB-231 (triple-negative breast cancer cell line), MCF-7 (human breast cancer cell line), A549 (lung carcinoma epithelial cells' cell line), B16-F10 (cell line of murine melanoma), HOC313 (human oral squamous-cell-carcinoma cell line), HSC3 (human oral squamous carcinoma cell line), SKBR3 (human breast cancer cell line), HeLa (HeLa Cell line), CIK (Cytokine-induced killer cells), C57BL/6 (Inbred strain of laboratory mouse), and PC3 (Prostate cancer cell line)

Shape	Coating and load	Targeting Agent	Target	Size (nm)	PTT Laser Wavelength (nm)	Cancer cell line	Temperature (℃)	Cancer type (Indication)	Reference
AuNC	-	Anti-HSP monoclonal antibody	HSP70	61.2 ± 4.85	808	4T1 and Female BALB mice	-	Breast	[59]
AuNR	-	Anti-EGFR antibody	EGFR	-	808	U373-MG and 1321N1	-	Glioblastoma	[66]
	-	Anti-EGFR antibody	EGFR	10 × 40	808	MDA-MB-231	T_{max} = 43	Breast	[67]
	-	Anti-HER2 antibody and HA	HER2 and CD44	55.1 × 14.1	808	MCF-7 and MCF-7 tumour bearing mice	≈ 55	Breast	[60]
	-	Anti-EGFR antibody	EGFR	40	850	A549	-	Lung	[68]
	Coated with BSA	R837	DCs, CD8+ T cells	122.1	1064	B16-F10	-	Melanoma	[69]

AuNSH	Coated with PLGA	Anti-HER2 antibody	EGF/HER-2/CD133 antibody	248.3	808	SKBR3 and MDA-MB-231	-	Breast	[70]
	Chitosan-layered, Paclitaxel loaded	Anti-EGFR antibody	EGFR	9	808	HeLa and MDA-MB-231 cells/ MDA-MB-231 tumour-bearing mice	T_{max} = 52.5	Breast	[71]
AuNST	ICG	Anti-HER2 antibody (Trastuzumab)	EGF/HER-2/CD133 antibody	135.3	808	CIK cells, SKBR3 / C57BL/6 and BALB/c nude mice	-	Breast	[72]
	-	Anti-CD33 antibody	EGF/HER-2/CD133 antibody	120	808	PC3 cell-line / male BALB/c athymic nude mice	-	Prostate	[61]

Diverse types of gold nanoparticles were utilised in various articles that we examined (Supplementary Table 1). One of the most utilised shapes of gold nanoparticles was AuNR followed by AuNST, AuNP, and AuNC (Figure 1). However, it was noted that a large number of the AuNPs that do not utilise mAbs were coated or had alternative surface modifications.

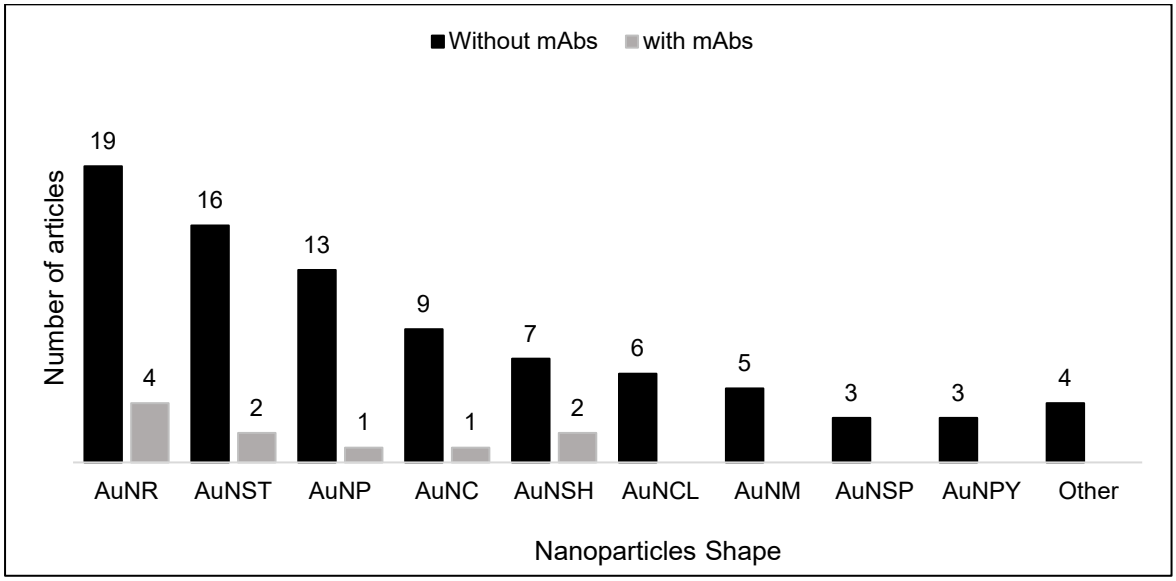

Figure 1 – Number of examined publications utilising AuNPs classified by shape.
AuNR (gold nanorod), AuNST (gold nano star), AuNP (gold nanoparticles), AuNC (Gold Nanocages), AuNSH (gold nano shell), AuNCL (Gold Nanoclusters), AuNM (Gold Nanomaterials), AuNSP (Gold Nanospheres), and AuNPY (Gold Nanopyrmids). Other include one article for each of the AuNU (Gold Nanourchins), AuNPR (Gold Nanoprisims), AuNF (Gold Nanoflower), and AuND (Gold Nanodumbless). The articles were covering the period 2015-2022, as summarised in Supplementary Table 1 and Table 1.

One of the common surface modifications is polyethylene glycol (PEG). In 13 AuNPs, PEG utilisation is linked to its ability in improving the distribution of the AuNP throughout the blood circulation [73]. Other platforms tended to assist the AuNPs by using mesoporous silica as a coating agent, because it possesses favourable biocompatibility, thermal stability, and desirable chemical properties. As drug carriers, they facilitate the effective loading and subsequent controlled release of the drugs to

the target sites [74]. The use of hyaluronic acid (HA) as a coating agent has also proved its efficacy in multiple studies [60]. The combination of AuNPs and HA increases the mobility of the AuNPs, resulting in a better distribution over the cancer site. Other articles have implemented the use of polyethyleneimine (PEI), as it is the most widely used cationic polyelectrolyte for preparing positively charged AuNPs. They feature dual roles as stabilising/reducing agents for gold ions and its chemical stability [75].

Most of the AuNPs analysed were studying the efficacy and safety in breast cancer, followed by lung, cervical and colon cancers (Figure 2). This focus is interestingly reflecting the incidents of these types of cancer. In addition, breast cancer is associated with challenges like treatment-related adverse events, poor outcomes in triple-negative breast cancer and balancing the treatment with quality of life [76]. The use of AuNPs might be crucial treatment option due to breast cancer high prevalence and the increased focus on localised treatment methods of non-invasive nature.

Huang et al. prepared gold nanorods that are conjugated to antibodies to specifically bind to the cancer cells before exposing these nanoparticles to continuous red laser at 800 nm to photothermally induce cancer cells killing [8]. However, gold nanoparticles suffer from some limitations in terms of their long exposure toxicity and their relatively weak optical signal [12].

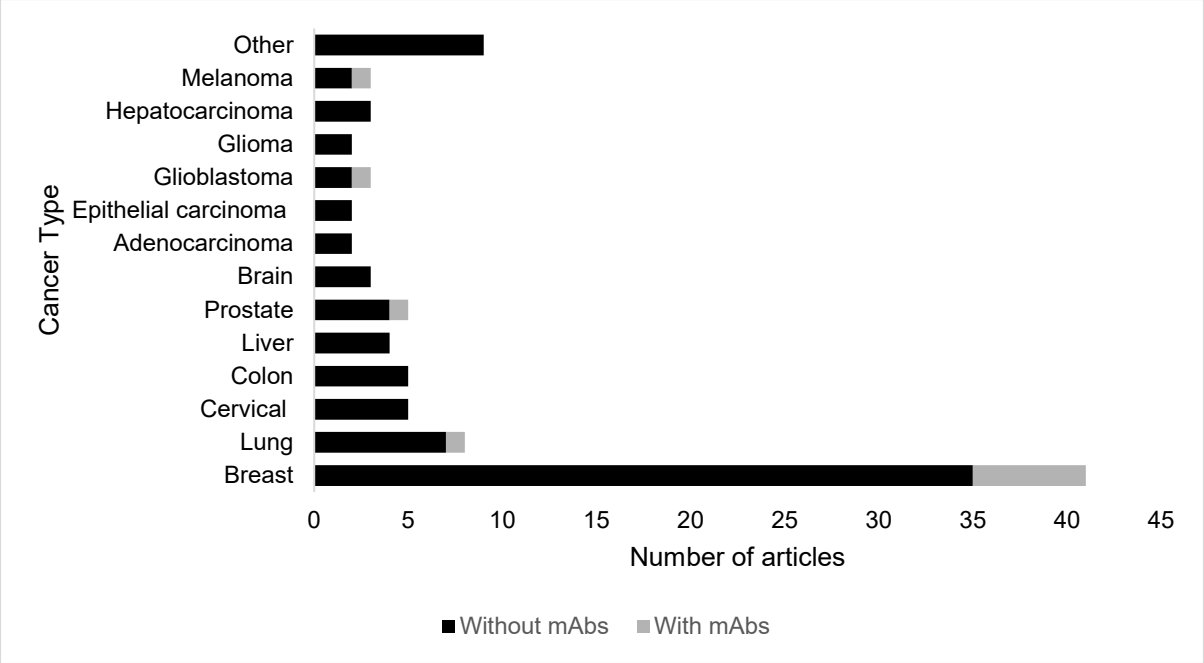

Figure 2: **Number of publications classified by cancer type.**
The articles covered wide range of cancers. Other include one article focusing on squamous cell, squamous vulvar, osteosarcoma, sarcoma, hepatoma, gastric, lymphoma, and pancreas cancers. The articles were covering the period 2015-2022, as summarised in Supplementary Table 1 and Table 1.

The role of membrane transporters in PTT

Membrane transporter proteins, which transport drug substances, are usually referred to as drug transporters in biomedical sciences. Two major families of membrane transport proteins are the ATP binding cassette (ABC) family and solute carrier (SLC) family. Solute carriers mediate the transport of ions or other solutes including vitamins, minerals, peptides, toxins, as well as numerous drug substances across cell membranes [77,78]. ABC transporters efflux molecules from the cell membrane in a process requiring energy in the form of ATP [77,79]; while SLC are both cellular influx and efflux carriers not directly dependent on ATP use, but often utilise the ion gradient across the cell membrane found for e.g. Na^+ or H^+ [80]. In human, membrane proteins are expressed in different tissues and organs such as the intestine, liver, kidney, blood

brain barrier, and testes [81]. Importantly, ABC transporters were found to be highly expressed in cancer cells which may lead to efflux of diverse structurally and mechanistically unrelated anticancer drug substances, and this is a major cause of multidrug resistance [82,83]. ABC transporters of importance in multidrug resistance are mainly permeability glycoprotein 170 (P-glycoprotein, P-gp which is encoded by the *ABCB1* gene), multidrug resistance-associated protein 1 (MRP1, encoded by *ABCC1*) and breast cancer resistance protein (BCRP, encoded by *ABCG2*) [82–85].

Recently, photothermal therapy used in cancer treatment was found to influence the expression of membrane transporters through the effect of hyperthermia which may either denaturate membrane transporters such as P-gp and MRP1, or increased the expression of heat shock factor-1 (HSF-1) which in turn decreased the expression of membrane transporters in cancer cells [13,14,16]. In addition, the substantial progress in designing nanoparticles that may accommodate different types of molecules such as anticancer drug substances, surfactants, and biological materials such as RNA and monoclonal antibody, enabled nanoparticles containing a photothermal agent and a membrane transporter modulator. These nanoparticles have been investigated *in vitro* and *in vivo* [17,86–88].

Nanoparticles for photothermal effect and modulation of membrane transporters *in vitro*

In order to obtain a synergistic effect of ablating the cancer cells and reversing the multidrug resistance related to overexpression of ABC transporters, different methods were utilised to modulate membrane transporter abundance. Molecules or biological materials that have been combined with photothermal nanoparticles include: 1) Photothermal agent which produce heat when exposed to NIR light and the released heat may decrease the expression of membrane transporters such as P-gp [13] and

MRP1 [14], or induce P-gp denaturation [15], 2) P-gp monoclonal antibody [87], 3) Nonionic surfactant such as Pluronic P123 and TPGS [17,86], 4) siRNA to downregulate the expression of a membrane transporter protein [18,88], 5) Nitric oxide donor molecule to liberate nitric oxide which decrease the expression of membrane transport proteins [89,90], 6) Natural product with specific P-gp inhibitory properties such as curcumin [91], and 7) Combination of different methods (Table 2).

Table 2: Nanoparticles for photothermal therapy and modulation of membrane transporters *in vitro* and *in vivo*.

N,N′-di-sec-butyl-N,N′-dinitroso-1,4-phenylenediamine (BNN6, Nitric oxide donor agent) , cypate-conjugated poly(ethylene glycol)-block-poly(diisopropanolamino ethyl methacrylate) (PEG- b -PDPA) diblock copolymer, D-α-tocopheryl polyethylene glycol 1000 succinate (TPGS), A549 (non-small cell lung cancer cell line), A549R (multidrug resistant variant of A549 cells), MCF-7 breast cancer cells, Adriamycin resistant cell line of MCF-7 (MCF-7/ADR), Vincristine-resistant human gastric cancer cell line (SGC7901/VCR), Hepatocellular carcinoma (HCC), Tumor inhibitory rate (TIR), HepG-2 cells (human hepatoma cells).

Nanoparticlecomponents	**Targeted transporter**	**Transporter substrate**	**Transporter modulator**	**Effect of transporter modulator *in vitro***	**Effect of nanoparticle + NIR light *in vivo***	**Reference**
Gold, Silicon dioxide, doxorubicin	P-gp	Doxorubicin	Hyperthermic effect	Hyperthermia increased the expression of heat shock factor-1 (HSF-1). HSF-1 depressed the expression of P-gp on cell membrane of MCF-7/ADR cells.		[13]
Cyanine dye, Cisplatin prodrug	MRP1	Cisplatin prodrug	Hyperthermic effect	Hyperthermia inhibited the expression of MRP1 and enhanced the cytotoxicity in A549 cells and resistant A549R cells.	Successful ablation of A549R tumor and A549 tumor in mice without regrowth, and no effect on other organs.	[14]
Oxidized carbon nanohorns, PEG, etoposide, P-gp monoclonal antibody	P-gp	Etoposide	P-gp monoclonal antibody	P-gp inhibited by direct interaction between the antibody and P-gp. Decrease the cellular efflux of etoposide in A549 and A549R cells.	Significant reduction of relative tumor volume (RTV) in A549R tumor-bearing mice.	[87]

Polydopamine, doxorubicin, PEG, folic acid, P-gp siRNA	P-gp	Doxorubicin	P-gp siRNA	P-gp expression was downregulated by 57% in MCF-7/ADR cells.	Significant reduction in tumor volume and weight in mice bearing MCF-7/ADR tumor.	88
Polydopamine, black phosphorus, doxorubicin, P-gp siRNA, PEG, aptamers	P-gp	Doxorubicin	P-gp siRNA	P-gp expression decreased by 68% and the cellular efflux of doxorubicin decreased, thus the cytotoxicity improved in MCF-7 and MCF-7/ADR cells.	Significant tumor ablation in MCF-7/ADR tumor-bearing nude mice, and no effect on other organs.	18
IR820 dyes, doxorubicin, Porous silicon attached with amine group.	P-gp	Doxorubicin	Hyperthermic effect	Hyperthermia induced P-gp denaturation in MCF-7 cells and MCF-7/ADR cells.		15
P-Cypate, doxorubicin, Pluronic P123	P-gp	Doxorubicin	Pluronic P123, Hyperthermic effect	Pluronic P123 inhibited P-gp activation by depleting ATP production in MCF-7/ADR. Hyperthermia increased the expression of HSF-1, which in turn depressed the expression of P-gp.	Tumor growth was completely inhibited in MCF-7/ADR tumor-bearing mice.	86
Polydopamine, Doxorubicin, TPGS	P-gp	Doxorubicin	TPGS	The cytotoxicity of doxorubicin increased by TPGS due to P-gp inhibition effect in MCF-7/ADR cells. It was suggested that TPGS reduced the		92

				transmembrane potential of mitochondria and consequently inhibited the ATP-production activity.		
Indocyanine green, Doxorubicin, TPGS	P-gp	Doxorubicin	TPGS	TPGS inhibited P-gp expression and enhanced the cytotoxicity of doxorubicin inSCG7901/VCR cells.		93,94
Polydopamine, 12-aminododecanoic, BNN6, doxorubicin, TPGS- Galactose	P-gp MRP3	Doxorubicin Rhodamine 123	TPGS Nitric oxide	Nitric oxide decreased the expression of P-gp and MRP3 in HepG2/ADR cells. TPGS decreased the intracellular ATP content and P-gp expression on cell membrane, and this inhibited P-gp and enhanced doxorubicin accumulation in the cells.	Inhibited the tumor growth in HepG2/ADR- tumor-bearing mice. Significant reduction in tumor weight without affecting the body weight of the mice.	17
Indocyanine green, curcumin, molybdenum disulfide	P-gp		Curcumin	Nanoparticles containing curcumin inhibited the expression of P-gp in HepG-2 cells.	Tumor volume and weight reduced significantly in hepatocellular carcinoma H22 tumor-bearing mice.	95
Copper selenide, N-diazeniumdiolate, doxorubicin	P-gp	Doxorubicin	Nitric oxide	The released nitric oxide gas inhibited P-gp expression by (≈ 40%) in MCF-7/ADR cells.	Tumor growth was completely inhibited (TIR = 100%), with no side effects on other organs.	89

N-doped graphene oxide (N-GO), BNN6, mitoxantrone	P-gp	Mitoxantrone	Nitric oxide	The released nitric oxide gas inhibited P-gp expression on the membrane of MCF-7/ADR cells	Significant decrease in tumor volume in MCF-7/ARD tumor-bearing nude mice without side effects on other organs.	[90]

Wang and co-workers used gold nanoparticles which were loaded with the anticancer drug substance doxorubicin (P-gp substrate) [13]. They found that hyperthermia increased the expression ofHSF-1 which depressed the expression of P-gp, thus decreased the efflux of doxorubicin and enhanced the cytotoxic effect in MCF-7/ADR cells [13]. When cyanine dye-loaded nanoparticles were exposed to NIR laser irradiation, the ensuing hyperthermia was found to decrease the expression of MRP1, thus increasing cisplatin-prodrug cytotoxicity in A549 and A549R cells, and enhancing the ablation effect of the nanoparticles [14].

Previous research has also reported that hyperthermia decreased MRP1 expression in HeLaMRP1 cells [16]. In addition, P-gp monoclonal antibodies were included in oxidized carbon nanoparticles to reverse P-gp activity and to decrease etoposide (P-gp substrate) efflux in A549 and A549R cells [87]. Beside the photothermal effect mediated by oxidized carbon nanohorns, utilisation of the P-gp monoclonal antibody suppressed the efflux activity of P-gp and increased the intracellular concentration of etoposide, and enhanced the cytotoxic effect of the nanoparticles [87].

Zeng et. al. [18] were able to augment the photothermal effect of polydopamine-modified black phosphorus by inclusion of doxorubicin (P-gp substrate) and P-gp siRNA in nanosheets. P-gp siRNA downregulated P-gp and enhanced the anticancer cytotoxicity in MCF-7 and MCF-7/ADR cells. Moreover, Cheng et al. [88] included a P-gp siRNA in polydopamine nanoparticles decorated with folic acid and these nanoparticles showed outstanding photothermal effect, P-gp downregulation, and a selective cell targeting ability mediated by the presence of folic acid in the formulation.

Nonionic surfactants which were shown to inhibit P-gp *in vitro* and *in vivo* [96–100] were included in the design of photothermal nanoparticles [86,93]. TPGS is a nonionic surfactant with P-gp inhibitory properties [101] and was included in nanoparticles containing a photothermal agent indocyanine green, and doxorubicin [93]. In the latter study, it was shown that TPGS decreased the expression of P-gp and enhanced the cytotoxicity of doxorubicin in SGC7901/VCR cells [93]. To potentiate the photothermal effect of nanoparticles, inclusion of several molecules to inhibit membrane transporter activities were also investigated. Du et al. included TPGS and nitric oxide donor molecule ((N,N′-di-sec-butyl-N,N′-dinitroso-1,4-phenylenediamine, (BNN6)) in polydopamine/doxorubicin nanoparticles [17]. TPGS and the released nitric oxide decrease P-gp and MRP3 expression, and reduced intracellular ATP content, thus enhanced intracellular doxorubicin, and increased the cytotoxicity in HCC cells. Other studies reported using nitric oxide donor molecules as P-gp modulators in order to enhance the photothermal effect of nanoparticles [89,90]. In these studies, nitric oxide decrease the expression of P-gp on MCF-7 and MCF-7/ADR cells, thus reversed multidrug resistance and potentiated the effect of anticancer drug substances included in the nanoparticles, consequently the photothermal effect was augmented [89,90].

Nanoparticles for photothermal effect and modulation of membrane transporters *in vivo*

In vivo studies were conducted in mice to compare the effect of multifunctional nanoparticles in the presence or absence of NIR light (Table 2). In these studies, researchers designed and characterized nanoparticles containing a photothermal agent, membrane transporter modulator, and/or a chemotherapeutic agent. Membrane transporter modulators used in *in vivo* studies were nonionic surfactants, siRNA, monoclonal antibody, and/or nitric oxide donor compounds to reverse

multidrug resistance in tumors [14,17,18,86,87,89,90,95]. Xenograft tumors were implanted into mice to investigate the effect of the multifunctional nanoparticles, with or without NIR light, on tumor volume, and the overall tumor growth in animals. Several studies showed significant reduction in tumor volume and weight in mice treated with nanoparticles and exposed to NIR laser compared to control (without laser exposure) (Table 2) [14,17,18,86,87,89,90,95]. Histopathological studies were also performed to assess the effect of nanoparticles components on other tissues and no side effects were reported on other organs such as heart, liver, and kidneys [14,17,18,86,87,89,90,95].

Pharmacokinetic studies conducted in Sprague Dawley rats showed prolonged systemic circulation time of photothermal nanoparticles in blood compared to circulation of anticancer drug substances not loaded in nanoparticles [18,88]. The prolonged circulation time may increase the exposure of photothermal agents and anticancer drug substances to the tumor sites, enhance the uptake of the nanoparticles by the tumors, and achieve a maximum inhibition of cancer growth. Interestingly, one study reported a 152 and 12 -fold increase in the maximal plasma concentration (C_{max}) and in the area under the plasma concentration time profile (AUC), respectively, in rats received intravenous P-cypate micellar formulation containing doxorubicin compared to control (rats receiving doxorubicin only) [86]. After intravenous administration a single dose of polydopamine nanoparticles containing doxorubicin, researchers reported a prolonged blood circulation of doxorubicin administered in the nanoparticles formulation noted as a seven-fold increase in half-life ($t½$) compared to rats received equivalent dose of free doxorubicin [17]. The results from these preclinical studies in animals indicated a promising future for photothermal therapy when included in multifunctional nanoparticles to simultaneously reverse multidrug resistance by membrane transporter modulation and ablate human tumors.

Conclusions:

Photothermal therapy seems a promising approach to treat patients with cancer diseases in the future. Gold nanoparticles are the most utilised type of nanoparticles in PTT. Targeting cancer by conjugating the PTT nanoparticles with monoclonal antibodies or by alternative coatings enhances the therapeutic efficacy of the PTT approach. In addition, inclusion of membrane transporter modulators in PTT nanoparticles enhanced the efficacy of the formulation *in vitro* and *in vivo.* It seems that the current advancement in designing multifunctional nanoparticles will assist researchers to create more effective and safe nanoparticles for PTT by inclusion of different substances in the formulation, with each having a specific role in the treatment of cancer diseases. However, many studies currently investigating the effect of PTT in cell cultures and animal models require follow-on pre-clinical and clinical trials to confirm the overall efficacy in humans.

References:

1. WHO. Cancer. Published February 2022. Accessed December 27, 2022. https://www.who.int/news-room/fact-sheets/detail/cancer

2. Siegel RL, Miller KD, Fuchs HE, Jemal A. Cancer statistics, 2022. *CA Cancer J Clin*. 2022;72(1):7-33. doi:10.3322/caac.21708

3. Macmillan Cancer Support. *Statistics Fact Sheet*.; 2022. https://www.macmillan.org.uk/dfsmedia/1a6f23537f7f4519bb0cf14c45b2a629/9468-10061/2022-cancer-statistics-factsheet

4. Yabroff KR, Wu XC, Negoita S, et al. Association of the COVID-19 Pandemic With Patterns of Statewide Cancer Services. *J Natl Cancer Inst*. 2022;114(6):907-909. doi:10.1093/jnci/djab122

5. Nurgali K, Jagoe RT, Abalo R. Editorial: Adverse Effects of Cancer Chemotherapy: Anything New to Improve Tolerance and Reduce Sequelae? *Front Pharmacol*. 2018;9:245. doi:10.3389/fphar.2018.00245

6. Majeed H, Gupta V. Adverse Effects Of Radiation Therapy. In: *StatPearls*. StatPearls Publishing; 2022. Accessed December 27, 2022. http://www.ncbi.nlm.nih.gov/books/NBK563259/

7. Han HS, Choi KY. Advances in Nanomaterial-Mediated Photothermal Cancer Therapies: Toward Clinical Applications. *Biomedicines*. 2021;9(3):305. doi:10.3390/biomedicines9030305

8. Huang X, El-Sayed IH, Qian W, El-Sayed MA. Cancer Cell Imaging and Photothermal Therapy in the Near-Infrared Region by Using Gold Nanorods. *J Am Chem Soc*. 2006;128(6):2115-2120. doi:10.1021/ja057254a

9. Al Qaraghuli MM. Biotherapeutic Antibodies for the Treatment of Head and Neck Cancer: Current Approaches and Future Considerations of Photothermal Therapies. *Front Oncol*. 2020;10:2710. doi:10.3389/fonc.2020.559596

10. Li X, Lovell JF, Yoon J, Chen X. Clinical development and potential of photothermal and photodynamic therapies for cancer. *Nat Rev Clin Oncol*. 2020;17(11):657-674. doi:10.1038/s41571-020-0410-2

11. Yang K, Zhao S, Li B, Wang B, Lan M, Song X. Low temperature photothermal therapy: Advances and perspectives. *Coord Chem Rev*. 2022;454:214330. doi:10.1016/j.ccr.2021.214330

12. Gupta N, Malviya R. Understanding and advancement in gold nanoparticle targeted photothermal therapy of cancer. *Biochim Biophys Acta BBA - Rev Cancer*. 2021;1875(2):188532. doi:10.1016/j.bbcan.2021.188532

13. Wang L, Lin X, Wang J, et al. Novel Insights into Combating Cancer Chemotherapy Resistance Using a Plasmonic Nanocarrier: Enhancing Drug Sensitiveness and Accumulation Simultaneously with Localized Mild Photothermal Stimulus of Femtosecond Pulsed Laser. *Adv Funct Mater*. 2014;24(27):4229-4239. doi:10.1002/adfm.201400015

14. Li Y, Deng Y, Tian X, et al. Multipronged Design of Light-Triggered Nanoparticles To Overcome Cisplatin Resistance for Efficient Ablation of Resistant Tumor. *ACS Nano*. 2015;9(10):9626-9637. doi:10.1021/acsnano.5b05097

15. Xia B, Zhang Q, Shi J, Li J, Chen Z, Wang B. Co-loading of photothermal agents and anticancer drugs into porous silicon nanoparticles with enhanced chemo-photothermal therapeutic efficacy to kill multidrug-resistant cancer cells. *Colloids Surf B Biointerfaces*. 2018;164:291-298. doi:10.1016/j.colsurfb.2018.01.059

16. Souslova T, Averill-Bates DA. Multidrug-resistant hela cells overexpressing MRP1 exhibit sensitivity to cell killing by hyperthermia: interactions with etoposide. *Int J Radiat Oncol Biol Phys*. 2004;60(5):1538-1551. doi:10.1016/j.ijrobp.2004.07.686

17. Du Z, Mao Y, Zhang P, et al. TPGS–Galactose-Modified Polydopamine Co-delivery Nanoparticles of Nitric Oxide Donor and Doxorubicin for Targeted Chemo–Photothermal Therapy against Drug-Resistant Hepatocellular Carcinoma. *ACS Appl Mater Interfaces*. 2021;13(30):35518-35532. doi:10.1021/acsami.1c09610

18. Zeng X, Luo M, Liu G, et al. Polydopamine-Modified Black Phosphorous Nanocapsule with Enhanced Stability and Photothermal Performance for Tumor Multimodal Treatments. *Adv Sci*. 2018;5(10):1800510. doi:10.1002/advs.201800510

19. Thakor AS, Gambhir SS. Nanooncology: the future of cancer diagnosis and therapy. *CA Cancer J Clin*. 2013;63(6):395-418. doi:10.3322/caac.21199

20. Obeid MA, Tate RJ, Mullen AB, Ferro VA. Lipid-based nanoparticles for cancer treatment. In: Grumezescu AM, ed. *Lipid Nanocarriers for Drug Targeting*. Elsevier; 2018:313-359. doi:10.1016/B978-0-12-813687-4.00008-6

21. Song S, Qin Y, He Y, Huang Q, Fan C, Chen HY. Functional nanoprobes for ultrasensitive detection of biomolecules. *Chem Soc Rev*. 2010;39(11):4234-4243. doi:10.1039/c000682n

22. Zhang Y, Li M, Gao X, Chen Y, Liu T. Nanotechnology in cancer diagnosis: progress, challenges and opportunities. *J Hematol OncolJ Hematol Oncol*. 2019;12(1):137. doi:10.1186/s13045-019-0833-3

23. Wu J. The Enhanced Permeability and Retention (EPR) Effect: The Significance of the Concept and Methods to Enhance Its Application. *J Pers Med*. 2021;11(8):771. doi:10.3390/jpm11080771

24. Sangboonruang S, Semakul N, Obeid MA, et al. Potentiality of Melittin-Loaded Niosomal Vesicles Against Vancomycin-Intermediate Staphylococcus aureus and Staphylococcal Skin Infection. *Int J Nanomedicine*. 2021;16:7639-7661. doi:10.2147/IJN.S325901

25. Aljabali AAA, Obeid MA. Inorganic-organic Nanomaterials for Therapeutics and Molecular Imaging Applications. *Nanosci Nanotechnol-Asia*. 10(6):748-765.

26. Alyamani H, Obeid MA, Tate RJ, Ferro VA. Exosomes: fighting cancer with cancer. *Ther Deliv*. 2019;10(1):37-61. doi:10.4155/tde-2018-0051

27. Hansen AE, Petersen AL, Henriksen JR, et al. Positron Emission Tomography Based Elucidation of the Enhanced Permeability and Retention Effect in Dogs with Cancer Using Copper-64 Liposomes. *ACS Nano*. 2015;9(7):6985-6995. doi:10.1021/acsnano.5b01324

28. Wong AD, Ye M, Ulmschneider MB, Searson PC. Quantitative Analysis of the Enhanced Permeation and Retention (EPR) Effect. *PLOS ONE*. 2015;10(5):e0123461. doi:10.1371/journal.pone.0123461

29. Obeid MA, Gany SAS, Gray AI, Young L, Igoli JO, Ferro VA. Niosome-encapsulated balanocarpol: compound isolation, characterisation, and cytotoxicity evaluation against human breast and ovarian cancer cell lines. *Nanotechnology*. 2020;31(19):195101. doi:10.1088/1361-6528/ab6d9c

30. Obeid MA, Alyamani H, Amawi H, et al. siRNA Delivery to Melanoma Cells with Cationic Niosomes. *Methods Mol Biol Clifton NJ*. 2021;2265:621-634. doi:10.1007/978-1-0716-1205-7_42

31. Matsumoto Y, Nichols JW, Toh K, et al. Vascular bursts enhance permeability of tumour blood vessels and improve nanoparticle delivery. *Nat Nanotechnol*. 2016;11(6):533-538. doi:10.1038/nnano.2015.342

32. Xie Z, Fan T, An J, et al. Emerging combination strategies with phototherapy in cancer nanomedicine. *Chem Soc Rev*. 2020;49(22):8065-8087. doi:10.1039/D0CS00215A

33. Elahi N, Kamali M, Baghersad MH. Recent biomedical applications of gold nanoparticles: A review. *Talanta*. 2018;184:537-556. doi:10.1016/j.talanta.2018.02.088

34. Zhang W, Wang F, Wang Y, et al. pH and near-infrared light dual-stimuli responsive drug delivery using DNA-conjugated gold nanorods for effective treatment of multidrug resistant cancer cells. *J Control Release Off J Control Release Soc*. 2016;232:9-19. doi:10.1016/j.jconrel.2016.04.001

35. Aljabali AAA, Zoubi MSA, Al-Batanyeh KM, et al. Gold-coated plant virus as computed tomography imaging contrast agent. *Beilstein J Nanotechnol*. 2019;10:1983-1993. doi:10.3762/bjnano.10.195

36. Dykman L, Khlebtsov N. Gold nanoparticles in biomedical applications: recent advances and perspectives. *Chem Soc Rev*. 2012;41(6):2256-2282. doi:10.1039/C1CS15166E

37. Chen J, Ning C, Zhou Z, et al. Nanomaterials as photothermal therapeutic agents. *Prog Mater Sci*. 2019;99:1-26. doi:10.1016/j.pmatsci.2018.07.005

38. Zhu X, Feng W, Chang J, et al. Temperature-feedback upconversion nanocomposite for accurate photothermal therapy at facile temperature. *Nat Commun*. 2016;7:10437. doi:10.1038/ncomms10437

39. Huang X, El-Sayed MA. Gold nanoparticles: Optical properties and implementations in cancer diagnosis and photothermal therapy. *J Adv Res*. 2010;1(1):13-28. doi:10.1016/j.jare.2010.02.002

40. Li J, Xie C, Huang J, Jiang Y, Miao Q, Pu K. Semiconducting Polymer Nanoenzymes with Photothermic Activity for Enhanced Cancer Therapy. *Angew Chem Int Ed*. 2018;57(15):3995-3998. doi:10.1002/anie.201800511

41. Fu S, Man Y, Jia F. Photothermal Effect of Superparamagnetic Fe_3O_4 Nanoparticles Irradiated by Near-Infrared Laser. *J Nanomater*. 2020;2020:e2832347. doi:10.1155/2020/2832347

42. Chu M, Shao Y, Peng J, et al. Near-infrared laser light mediated cancer therapy by photothermal effect of Fe3O4 magnetic nanoparticles. *Biomaterials*. 2013;34(16):4078-4088. doi:10.1016/j.biomaterials.2013.01.086

43. Sun Z, Xie H, Tang S, et al. Ultrasmall Black Phosphorus Quantum Dots: Synthesis and Use as Photothermal Agents. *Angew Chem Int Ed*. 2015;54(39):11526-11530. doi:10.1002/anie.201506154

44. Liang C, Diao S, Wang C, et al. Tumor Metastasis Inhibition by Imaging-Guided Photothermal Therapy with Single-Walled Carbon Nanotubes. *Adv Mater*. 2014;26(32):5646-5652. doi:10.1002/adma.201401825

45. Yang K, Zhang S, Zhang G, Sun X, Lee ST, Liu Z. Graphene in Mice: Ultrahigh In Vivo Tumor Uptake and Efficient Photothermal Therapy. *Nano Lett*. 2010;10(9):3318-3323. doi:10.1021/nl100996u

46. Fan W, Bu W, Shen B, et al. Intelligent MnO2 Nanosheets Anchored with Upconversion Nanoprobes for Concurrent pH-/H2O2-Responsive UCL Imaging and Oxygen-Elevated Synergetic Therapy. *Adv Mater*. 2015;27(28):4155-4161. doi:10.1002/adma.201405141

47. Shao L, Zhang R, Lu J, Zhao C, Deng X, Wu Y. Mesoporous Silica Coated Polydopamine Functionalized Reduced Graphene Oxide for Synergistic Targeted Chemo-Photothermal Therapy. *ACS Appl Mater Interfaces*. 2017;9(2):1226-1236. doi:10.1021/acsami.6b11209

48. Cui G, He P, Yu L, Wen C, Xie X, Yao G. Oxygen self-enriched nanoplatform combined with US imaging and chemo/photothermal therapy for breast cancer. *Nanomed*. 2020;29:102238. doi:10.1016/j.nano.2020.102238

49. Obeid MA, Teeravatcharoenchai T, Connell D, et al. Examination of the effect of niosome preparation methods in encapsulating model antigens on the vesicle characteristics and their ability to induce immune responses. *J Liposome Res*. 2021;31(2):195-202. doi:10.1080/08982104.2020.1768110

50. Aboeleneen SB, Scully MA, Harris JC, Sterin EH, Day ES. Membrane-wrapped nanoparticles for photothermal cancer therapy. *Nano Converg*. 2022;9(1):37. doi:10.1186/s40580-022-00328-4

51. Xu HL, Shen BX, Lin MT, et al. Homing of ICG-loaded liposome inlaid with tumor cellular membrane to the homologous xenografts glioma eradicates the primary focus and prevents lung metastases through phototherapy. *Biomater Sci*. 2018;6(9):2410-2425. doi:10.1039/C8BM00604K

52. Bianchi L, Mooney R, Cornejo YR, et al. Thermal analysis of laser irradiation-gold nanorod combinations at 808 nm, 940 nm, 975 nm and 1064 nm wavelengths in breast cancer model. *Int J Hyperthermia*. 2021;38(1):1099-1110. doi:10.1080/02656736.2021.1956601

53. Obeid MA, Al Qaraghuli MM, Alsaadi M, Alzahrani AR, Niwasabutra K, Ferro VA. Delivering natural products and biotherapeutics to improve drug efficacy. *Ther Deliv*. 2017;8(11):947-956. doi:10.4155/tde-2017-0060

54. Weiner LM, Surana R, Wang S. Antibodies and cancer therapy: versatile platforms for cancer immunotherapy. *Nat Rev Immunol*. 2010;10(5):317-327. doi:10.1038/nri2744

55. Zahavi D, Weiner L. Monoclonal Antibodies in Cancer Therapy. *Antibodies*. 2020;9(3). doi:10.3390/antib9030034

56. Hendriks D, Choi G, de Bruyn M, Wiersma VR, Bremer E. Chapter Seven - Antibody-Based Cancer Therapy: Successful Agents and Novel Approaches. In: Galluzzi L, ed. *International Review of Cell*

and Molecular Biology. Vol 331. Academic Press; 2017:289-383. doi:10.1016/bs.ircmb.2016.10.002

57. Jiang X, Wang J, Deng X, et al. The role of microenvironment in tumor angiogenesis. *J Exp Clin Cancer Res CR*. 2020;39:204. doi:10.1186/s13046-020-01709-5

58. Zheng X, Wang J, Rao J. Chapter 27 - The Chemistry in Surface Functionalization of Nanoparticles for Molecular Imaging. In: Ross BD, Gambhir SS, eds. *Molecular Imaging (Second Edition)*. Academic Press; 2021:493-516. doi:10.1016/B978-0-12-816386-3.00021-1

59. Cheng Y, Bao D, Chen X, et al. Microwave-triggered/HSP-targeted gold nano-system for triple-negative breast cancer photothermal therapy. *Int J Pharm*. 2021;593:120162. doi:10.1016/j.ijpharm.2020.120162

60. Xu W, Qian J, Hou G, et al. A dual-targeted hyaluronic acid-gold nanorod platform with triple-stimuli responsiveness for photodynamic/photothermal therapy of breast cancer. *Acta Biomater*. 2019;83:400-413. doi:10.1016/j.actbio.2018.11.026

61. Tan H, Hou N, Liu Y, et al. CD133 antibody targeted delivery of gold nanostars loading IR820 and docetaxel for multimodal imaging and near-infrared photodynamic/photothermal/chemotherapy against castration resistant prostate cancer. *Nanomedicine Nanotechnol Biol Med*. 2020;27:102192. doi:10.1016/j.nano.2020.102192

62. Bolaños K, Kogan MJ, Araya E. Capping gold nanoparticles with albumin to improve their biomedical properties. *Int J Nanomedicine*. 2019;14:6387-6406. doi:10.2147/ijn.S210992

63. Silva IO, Ladchumananandasivam R, Nascimento JHO, et al. Multifunctional Chitosan/Gold Nanoparticles Coatings for Biomedical Textiles. *Nanomaterials*. 2019;9(8):1064.

64. Essa D, Kondiah PPD, Choonara YE, Pillay V. The Design of Poly(lactide-co-glycolide) Nanocarriers for Medical Applications. *Front Bioeng Biotechnol*. 2020;8. doi:10.3389/fbioe.2020.00048

65. Thomas R, Weihua Z. Rethink of EGFR in Cancer With Its Kinase Independent Function on Board. *Front Oncol*. 2019;9. doi:10.3389/fonc.2019.00800

66. Fernández-Cabada T, Sánchez C, Pisarchyk L, Serrano Olmedo J, Ramos M. Optical Hyperthermia Using Anti-Epidermal Growth Factor Receptor-Conjugated Gold Nanorods to Induce Cell Death in Glioblastoma Cell Lines. *J Nanosci Nanotechnol*. 7AD;16:7689-7695. doi:10.1166/jnn.2016.12570

67. Zhang M, Kim HS, Jin T, Woo J, Piao YJ, Moon WK. Near-infrared photothermal therapy using anti-EGFR-gold nanorod conjugates for triple negative breast cancer. *Oncotarget*. 2017;8(49):86566-86575. doi:10.18632/oncotarget.21243

68. Knights O, Freear S, McLaughlan JR. Improving Plasmonic Photothermal Therapy of Lung Cancer Cells with Anti-EGFR Targeted Gold Nanorods. *Nanomaterials*. 2020;10(7):1307. doi:10.3390/nano10071307

69. Zhou B, Song J, Wang M, et al. BSA-bioinspired gold nanorods loaded with immunoadjuvant for the treatment of melanoma by combined photothermal therapy and immunotherapy. *Nanoscale*. 2018;10(46):21640-21647. doi:10.1039/C8NR05323E

70. Dong Q, Yang H, Wan C, et al. Her2-Functionalized Gold-Nanoshelled Magnetic Hybrid Nanoparticles: a Theranostic Agent for Dual-Modal Imaging and Photothermal Therapy of Breast Cancer. *Nanoscale Res Lett*. 2019;14(1):235. doi:10.1186/s11671-019-3053-4

71. Manivasagan P, Nguyen VT, Jun SW, et al. Anti-EGFR antibody conjugated thiol chitosan-layered gold nanoshells for dual-modal imaging-guided cancer combination therapy. *J Control Release Off J Control Release Soc*. 2019;311-312:26-42. doi:10.1016/j.jconrel.2019.08.007

72. Liang S, Sun M, Lu Y, et al. Cytokine-induced killer cells-assisted tumor-targeting delivery of Her-2 monoclonal antibody-conjugated gold nanostars with NIR photosensitizer for enhanced therapy of cancer. *J Mater Chem B*. 2020;8(36):8368-8382. doi:10.1039/D0TB01391A

73. Chen TY, Chen MR, Liu SW, et al. Assessment of Polyethylene Glycol-Coated Gold Nanoparticle Toxicity and Inflammation In Vivo Using NF-κB Reporter Mice. *Int J Mol Sci*. 2020;21(21). doi:10.3390/ijms21218158

74. Bharti C, Nagaich U, Pal AK, Gulati N. Mesoporous silica nanoparticles in target drug delivery system: A review. *Int J Pharm Investig*. 2015;5(3):124-133. doi:10.4103/2230-973x.160844

75. Cho TJ, Gorham JM, Pettibone JM, Liu J, Tan J, Hackley VA. Parallel multi-parameter study of PEI-functionalized gold nanoparticle synthesis for bio-medical applications: part 1—a critical assessment of methodology, properties, and stability. *J Nanoparticle Res*. 2019;21(8):188. doi:10.1007/s11051-019-4621-3

76. Lee J, Chatterjee DK, Lee MH, Krishnan S. Gold nanoparticles in breast cancer treatment: Promise and potential pitfalls. *Cancer Lett*. 2014;347(1):46-53. doi:10.1016/j.canlet.2014.02.006

77. Higgins CF. ABC transporters: physiology, structure and mechanism--an overview. *Res Microbiol*. 2001;152(3-4):205-210. doi:10.1016/s0923-2508(01)01193-7

78. Lee VHL. Membrane transporters. *Eur J Pharm Sci*. 2000;11:S41-S50. doi:10.1016/S0928-0987(00)00163-9

79. Dean M, Moitra K, Allikmets R. The human ATP-binding cassette (ABC) transporter superfamily. *Hum Mutat*. 2022;43(9):1162-1182. doi:10.1002/humu.24418

80. Hediger MA, Romero MF, Peng JB, Rolfs A, Takanaga H, Bruford EA. The ABCs of solute carriers: physiological, pathological and therapeutic implications of human membrane transport proteinsIntroduction. *Pflugers Arch*. 2004;447(5):465-468. doi:10.1007/s00424-003-1192-y

81. International Transporter Consortium, Giacomini KM, Huang SM, et al. Membrane transporters in drug development. *Nat Rev Drug Discov*. 2010;9(3):215-236. doi:10.1038/nrd3028

82. Gottesman MM, Fojo T, Bates SE. Multidrug resistance in cancer: role of ATP-dependent transporters. *Nat Rev Cancer*. 2002;2(1):48-58. doi:10.1038/nrc706

83. Szakács G, Paterson JK, Ludwig JA, Booth-Genthe C, Gottesman MM. Targeting multidrug resistance in cancer. *Nat Rev Drug Discov*. 2006;5(3):219-234. doi:10.1038/nrd1984

84. Bukowski K, Kciuk M, Kontek R. Mechanisms of Multidrug Resistance in Cancer Chemotherapy. *Int J Mol Sci*. 2020;21(9):3233. doi:10.3390/ijms21093233

85. Saraswathy M, Gong S. Different strategies to overcome multidrug resistance in cancer. *Biotechnol Adv*. 2013;31(8):1397-1407. doi:10.1016/j.biotechadv.2013.06.004

86. Yu H, Cui Z, Yu P, et al. pH- and NIR Light-Responsive Micelles with Hyperthermia-Triggered Tumor Penetration and Cytoplasm Drug Release to Reverse Doxorubicin Resistance in Breast Cancer. *Adv Funct Mater*. 2015;25(17):2489-2500. doi:10.1002/adfm.201404484

87. Wang J, Wang R, Zhang F, et al. Overcoming multidrug resistance by a combination of chemotherapy and photothermal therapy mediated by carbon nanohorns. *J Mater Chem B*. 2016;4(36):6043-6051. doi:10.1039/C6TB01469K

88. Cheng W, Nie J, Gao N, et al. A Multifunctional Nanoplatform against Multidrug Resistant Cancer: Merging the Best of Targeted Chemo/Gene/Photothermal Therapy. *Adv Funct Mater*. 2017;27(45):1704135. doi:10.1002/adfm.201704135

89. Wang J, Wu C, Qin X, et al. NIR-II light triggered nitric oxide release nanoplatform combined chemo-photothermal therapy for overcoming multidrug resistant cancer. *J Mater Chem B*. 2021;9(6):1698-1706. doi:10.1039/D0TB02626C

90. Huang X, Gu R, Zhong Z, et al. Nitric oxide-sensitized mitoxantrone chemotherapy integrated with photothermal therapy against multidrug-resistant tumors. *Mater Chem Front*. 2021;5(15):5798-5805. doi:10.1039/D1QM00523E

91. Lopes-Rodrigues V, Sousa E, Vasconcelos MH. Curcumin as a Modulator of P-Glycoprotein in Cancer: Challenges and Perspectives. *Pharm Basel Switz*. 2016;9(4):71. doi:10.3390/ph9040071

92. Xing Y, Zhang J, Chen F, Liu J, Cai K. Mesoporous polydopamine nanoparticles with co-delivery function for overcoming multidrug resistance via synergistic chemo-photothermal therapy. *Nanoscale*. 2017;9(25):8781-8790. doi:10.1039/C7NR01857F

93. Gao H, Bai Y, Chen L, Ei Fakhri G, Wang M. Self-Assembly Nanoparticles for Overcoming Multidrug Resistance and Imaging-Guided Chemo-Photothermal Synergistic Cancer Therapy . *Int J Nanomedicine*. 2020;15:809-819. doi:10.2147/IJN.S232449

94. Gao Q, Bao L, Mao H, et al. Rapid development of an inactivated vaccine candidate for SARS-CoV-2. *Science*. Published online May 6, 2020. doi:10.1126/science.abc1932

95. Li S, Yang S, Liu C, et al. Enhanced Photothermal-Photodynamic Therapy by Indocyanine Green and Curcumin-Loaded Layered MoS2 Hollow Spheres via Inhibition of P-Glycoprotein. *Int J Nanomedicine*. 2021;16:433-442. doi:10.2147/IJN.S275938

96. Lo Y li. Relationships between the hydrophilic-lipophilic balance values of pharmaceutical excipients and their multidrug resistance modulating effect in Caco-2 cells and rat intestines. *J Control Release Off J Control Release Soc*. 2003;90(1):37-48. doi:10.1016/s0168-3659(03)00163-9

97. Rege BD, Kao JPY, Polli JE. Effects of nonionic surfactants on membrane transporters in Caco-2 cell monolayers. *Eur J Pharm Sci Off J Eur Fed Pharm Sci*. 2002;16(4-5):237-246. doi:10.1016/s0928-0987(02)00055-6

98. Al-Ali AAA, Nielsen RB, Steffansen B, Holm R, Nielsen CU. Nonionic surfactants modulate the transport activity of ATP-binding cassette (ABC) transporters and solute carriers (SLC): Relevance to oral drug absorption. *Int J Pharm*. 2019;566:410-433. doi:10.1016/j.ijpharm.2019.05.033

99. Al-Ali AAA, Quach JRC, Bundgaard C, Steffansen B, Holm R, Nielsen CU. Polysorbate 20 alters the oral bioavailability of etoposide in wild type and mdr1a deficient Sprague-Dawley rats. *Int J Pharm*. 2018;543(1-2):352-360. doi:10.1016/j.ijpharm.2018.04.006

100. Al-Ali AAA, Steffansen B, Holm R, Nielsen CU. Nonionic surfactants increase digoxin absorption in Caco-2 and MDCKII MDR1 cells: Impact on P-glycoprotein inhibition, barrier function, and repeated cellular exposure. *Int J Pharm*. 2018;551(1-2):270-280. doi:10.1016/j.ijpharm.2018.09.039

101. Hanke U, May K, Rozehnal V, Nagel S, Siegmund W, Weitschies W. Commonly used nonionic surfactants interact differently with the human efflux transporters ABCB1 (p-glycoprotein) and ABCC2 (MRP2). *Eur J Pharm Biopharm Off J Arbeitsgemeinschaft Pharm Verfahrenstechnik EV*. 2010;76(2):260-268. doi:10.1016/j.ejpb.2010.06.008

Supplementary Table 1A: Summary of gold nanoparticles not containing monoclonal antibodies as targeted therapies.

Shape	Coating and/or Load	Target	Size (nm)	PTT Laser Wavelength (nm)	Cancer cells	Temperature (℃)	Cancer cell line (Indication)	Observation	Reference
AuNC	PEG coated; HA loaded	-	50.4	808	4T1 / 4T1 tumour-bearing mice	≈ 53	Breast	Rise of tumour temperature to ≈43.5°C decreasing tumour growth and caused 4T1 tumours regression for 21 days.	[1]
	Erythrocytes membrane vesicles, Paclitaxel and anti-EpCam loaded	-	40	808	4T1	≈ 49	Breast	Reduction of 4T1 cells viability to 40%, reaching 25% when combined with the Paclitaxel.	[2]
	HA Coated, Doxorubicin loaded	-	50	808	MDA-MB-231 and MDA-MB-231 tumour bearing mice	≈ 42	Breast	Tumour growth reduction after rise in tumour temperature to ≈44°C. Doxorubicin combination led to complete elimination in 9 days of MDA-MB-231 tumours.	[3]
	Surface modified with Poly (acrylic acid) and p(NIPAM-co-AM), Doxorubicin and Erlotinib loaded	EGFR	47.4	808	MCF-7 (Low EGFR) and A431 (High EGFR) cells/ MCF-7 and A431 tumour bearing mice	≈ 46	Squamous vulvar tumour and adenocarcinoma	PTT treatment led to a rise of temperature to ≈ 46.7°C reducing tumour growth. Erlotinib and doxorubicin combination caused MCF-7 tumours suppression for 9 days and promoted complete elimination of A431 in 6 days.	[4]

	Coated with MicroRNA-181b into PEI-modified and FR-targeted	-	50	808	SMMC-7721 / SMMC-7721 tumour-bearing mice	ΔT = 28.2	Hepatocellular carcinoma	Gene delivery system in combination with photothermal therapy will be of great potential use in future cancer therapy	5
	Anti-miR-181b	-	L: 42.3 ± 4.2 × W: 12.6 ± 2.1	808	MCF-7	-	Adenocarcinoma	Activation of photothermal and photodynamic therapeutic effect in MCF7 cells and tumour-bearing mice, possessing significant potential for cancer therapy	6
	-	-	70.5	808	4T1, Female BALB/c nude mice, female BALB/c mice	-	Breast	A promising delivery platform for breast cancer therapy	7
	Anginex	-	39 ± 3	808	4 T1	< 40	Breast	Cell death of tumour and endothelial cells	8
	Surface modified with PEG; Doxorubicin loaded	-	91.2	808	MCF-7 / ADR	-	Breast	Excellent exertion of anti-tumour effects under NIR irradiation	9
AuNCL	Hyaluronan-polycaprolactone co-polymer coated, Verteporfin loaded	-	150	808	MDA-MB-231 and MDA-MB-231 tumour bearing mice	≈ 74.1	Breast	Tumour temperature rise to 60°C assisting the suppression of growth for 21 days. Combination of PTT and Verteporfin caused complete elimination of MDA-MB-231 tumours.	10
	Surface modified with sodium alginate	-	24	660	KB and 293T / KB tumour-bearing mice	≈ 50	Epithelial carcinoma	Rise of the tumour temperature above 50°C resulting in thermal ablation of KB tumours	11

	Coated with hybrid albumin nanoparticles	-	Agglomeration average size of 4.4	808	HCT 116 / HCT 116 tumour-bearing mice	T_{max} = 70	Colon	The formulation presented can serve as a potential platform for optically visualizing and treating colon cancers.	12
	-	-	61.22 ± 2.63	808	4 T1	52.3 ± 2.3	Breast	Good excretion over time / effective tumour localisation and low toxicity	13
	Hyaluronidase	-	50	808	4 T1	77.8	Breast	Increased penetration and distribution into tumour tissue.	14
	-	Peptides	53	750	PANC1-CTSE / mice	-	Pancreatic	Significant therapeutic effects against pancreatic tumours as well as the decreased side effects in pancreas tissues	15
AuNCO	-	-	L: 50 ± 5 × W: 20 ± 2	808	MCF-7	56.2	Breast	Selective induction and of apoptosis for MCF-7 cells	16
AuND	-	-	L: 101.3 ± 5.8 × W: 19.1 ± 2.3	1064	MCF-7 and 4T1	50	Breast	Tumour growth suppression and host antitumour immunity stimulation, also presented good thermal stability, high photothermal conversion efficiency and high photoacoustic signals.	17
AuNF	Doxorubicin loaded	-	80-100	808	MCF-7	53	Breast	Adequate internalisation of nanoparticles to MCF-7 cells by endocytosis	18
AuNM	MnO2	-	25	808	4T1 / 4T1 tumour-bearing mice	42	Breast	Smart theragnostic nanoplatform for the diagnosis and effective treatment of cancer	19
	PEG-Ce6	-	42 ± 3	808	HeLa, L929, and U14 cell lines / U14	58.7	Cervical	Great potential and remarkable tumour specificity and improved therapy.	20

					tumour-bearing mice				
	HCNs	-	275 ± 0.35	808	CT26 / CT26 tumour bearing mice	52.9	Colon	Efficient tumour treatment platform, providing proof-of-concept tumour catalytic−photothermal therapy established on nanozymes	21
	Cu TPNCs	-	22.8 ± 4.6	808 and 1064	NIH3T3, KB and KB tumour-bearing mice	≈ 19.8	Epithelial carcinoma	Robust platform for multimodal photothermal therapy that is image-guided with symbolic therapeutic effects	22
	-	-	118	1064	HeLa, HeLa tumour-bearing mice	ΔT > 40	Cervical	Efficient approach of applying two-dimensional gold nanoplate core and TiO2 shell nanostructures as innovative nano-agents for advanced multifunctional anticancer in the second NIR window	23
AuNP	-	Lactoferrin (LF)	5	532	Human GBM U87MG cell line / Male BALB/c nude mice	-	Brain	Outstanding temperature increase in GBM and significant reduction of tumour volume under laser irradiation	24
	-	Folic Acid (FA)	10 ± 2	808	C6 glioma	-	Brain	Promising nanoprobes with targeting ability, cell tracking, and PTT effect	25
	Deoxyribonucleic acids	Aptamers	13	660	MCF-7, HeLa, L02 / female nude mice	-	Breast	Significant sensitivity and specificity, achieving real-time monitoring of the dynamic change in tumours during therapy	26

	Coated with Si	Folic Acid (FA)	25	810	MCF-7 and MDA-MB-231	-	Breast	Improved efficacy of laser therapy in breast cancer cell destruction	27
	-	-	85	808	4 T1	52	Breast	Improved tumour killing ability / Distinguished biosecurity in mice and 4T1 cells	28
	-	Peptides	L: 56.1 ± 0.3 × W: 62.8 ± 0.4	808	HUVEC and HCT-116 cell line/ female nude mice	-	Colon	Improved tumour accumulation and retention, activating the PA and PTT effect for sensitive imaging and competent therapy of tumours	29
	AS1411 and DNA modified	Aptamers	24.42	808	SW480	-	Colon	Potent cytotoxic effect and notably enhanced inhibition effect on cells proliferation to SW480 cells	30
	-	Glutathione coated	L: 239 ± 72 × W: 254 ± 64	760	HepG2	-	Liver	Effective cancer cell ablation	31
	-	Peptides	72.4	808	HCC-LM3 / nude mice	-	Liver	Excellent biocompatibility, high cancer cells absorption, notable inhibition of tumour growth	32
	-	Serum albumin (SA)	49	808	HepG2 and HepB5	-	Liver	increased intracellular uptake in liver cancer cells	33
	Coated with Mesoporous silica	Peptides	20	808	A540, HOB, and HMSC / mice	-	Lung	Enhanced cellular uptake by tumour cells. Exhibiting significant therapeutic efficacy on spinal tumour cells.	34
	CpG	-	AuNS (D: 50) and AuNR (L:	532 and 780	RAW264.7 and EG7-OVA	-	Lymphoma	The treatment symbolically retarded tumour growth and lengthened the survival	35

			38 × W: 10)		tumour-bearing mice				
	-	Peptides	13	650	PC-3, MCF-7 / male BALB/c nude mice	-	Prostate	AuNPs can be enzymatically massed into sizable aggregates and improve the temperature of the tumour	36
AuNPR	Ce6-Peptide	PD-L1	-	633	GCC827 and A549 / female BALB/c nude mice	-	Lung	Biocompatible and notably decrease tumour growth	37
AuNPY	HA	CD44	70.7 ±1.3	808	MDA-MB-231	62.7	Breast	Significant cell uptake by MDA-MB-231 and enhanced PTT efficacy	38
	-	-	L: 117.05 ± 4.45 × W: 36.08 ± 2.55	808	MCF-7	61	Breast	Cell viability reduction with relative volume of treated MCF-7 tumours	39
	-	-	75 × 27	808	MDA-MB-231	< 45	Breast	Good photoluminescence, optimal colloidal stability and no toxicity	40
AuNR	Surface modified with PEG and PLGA	-	L: 8 × W: 2	808	U87MG / U87MG tumour-bearing mice	≈ 75	Glioblastoma	Increase of temperature to 60°C excreting total ablation of U87MG tumours without recurrence from day 1 until day 16.	41
	Surface modified with Polysarcosine	-	L: 28 × W: 7.5	808	A549 / A549 tumour-bearing mice	≈ 90	Lung Adenocarcinoma	Increase of temperature to 63.6 °C excreting total ablation of A549 tumours without recurrence from day 1 until day 16	42
	Surface modified with Human serum albumin,	-	L: 30 × W: 10	808	SCC8 / SCC7 tumour bearing mice	≈ 55	Squamous Cell Carcinoma	a 25°C incline in the tumours' temperature, truncated Evans blue action promoted the complete elimination of SCC7 tumours.	43

	truncated Evans Blue								
	Coated with rabies virus mimetic silica	-	L: 79.9 × W: 20.1	808	N2a cells / N2a 176 tumour-bearing mice	T_{max} = 50	Brain	Passthrough to the brain by neuronal pathway bypassing the blood-brain barrier, and react to near-infrared laser irradiation, emit heat, and effectively suppress brain tumours.	[44]
	Surface modified with PEG	-	L: 104.6 × W:68.6	808	4T1 / 4T1 tumour-bearing mice	T_{max} = 45	Breast	Indicate excellent potential nanoplatforms for cancer diagnosis and therapy future	[45]
	Coated with Mesoporous silica, B-cyclodextrin as gatekeeper functionalised with lactobionic acid and PEG	-	L: 39.8 × W: 10.2	808	HepG2 and COS7 / HepG2 tumour-bearing mice	Tmax = 64.8 and 39.1	Hepatoma	Clear exhibition of near-infrared induced thermal effect, significantly improving the PDT and chemotherapy efficiency, resulting in a super additive effect.	[46]
	Surface modified with PEG-modified with phosphorylcholine and sulfobetaine	-	L: 28 × W: 7.5	808	HepG2 cells / KB tumour-bearing mice	ΔT = 30.7	Hepatoma	Induction of complete ablation of KB tumours, without observing tumour reoccurrence until 40 days	[47]
	MS coated, Indocyanine green, end-capped with B-cyclodextrin	-	L: 57.3 × W: 16.2	808	MCF-7 and MCF-7 tumour bearing mice	ΔT = 31.2	Breast	The composite nanoplatform provided good antitumour effect while minimising side effect.	[48]

	HA and SM	CD44 and acidity	-	808	MDA-MB-231	ΔT > 20	Breast	This multifunctional nano system provides potential platform for combined chemotherapy and photothermal cancer therapy.	49
	HA and FA	CD44 and FR	-	808	MCF-7	ΔT ≈ 30	Breast	Combined chemotherapy and photothermal therapy completely suppressed tumours without obvious systemic toxicity until 20 days of treatment.	50
	Ovalbumin assembled, CpG	DCs, CD8+ T cells	-	-	4T1	-	Breast	Importance of mild heat in inflecting the microenvironment for improved immunotherapy, by transforming the tumour into an in-situ vaccine.	51
	PEI and CpG	DCs, CD8+ T cells, CD4+ T cells	-	808	4T1	-	Breast	Promising nanoplatform for tumour therapy by combining with near infrared photothermal therapy and immunotherapy.	52
	Coated with cancer cell membranes, loaded with Doxorubicin	-	164.5 ± 0.7	-	4T1	-	Breast	Disruption of load release in the tumour targeting and immune escape abilities, affording a robust result of guided imaging PTT and chemotherapy.	53
	-	-	L: 70 × W: 20	808	MCF-7	78.7	Breast	Enhanced cell proliferative efficiency in breast cancer cells, increased blood circulation, enhanced tumour contraction and excretion of cancer cell apoptosis	54
	PLGA surface modified	Serum albumin (SA)	245.8	808	CT25 and MCF7	-	Colon	A promising combination therapy of PTT and chemotherapeutic effects without excreting unwanted side	55

								effects on a murine colon cancer animal model	
	CpG	-	-	808	H22	-	Hepatocarcinoma	The model can be utilized as efficient antitumour agent.	56
	-	Lactoferrin (LF)	L: 70 × W: 11.5	980	HepG2 / nude mice	-	Liver	Enhanced uptake and retention by cancer cell, the model showed total destruction of tumours cells without recurrence after one treatment	57
	BSA modified	Serum albumin (SA)	50	808	Lewis / female C56BL/6 mice	-	Lung	Outstanding biosafety without laser irradiation, and presented superior therapeutic effect on tumour cells due to the excellent tumour targeting and multi-stage AuNP delivery for deep tumour diffusion, that in return enhanced mice survival rate	58
	Surface modified with polyamidoamine dendrimer and RGD	-	L: 42 × W:10	808	A375 / a375 tumour bearing mice	-	Melanoma	Induced blood flow blockage in tumour tissue 3 hours after NIR laser irradiation and caused tumour growth reduction for 28 days	59
	-	Peptides	L: 52.33 ± 8.05 × W: 13.99 ± 1.09	808	PC3 / BALB/c athymic nude mice	-	Prostate	Demonstrated a significant PTT effect as well as enhanced thermodynamic therapy	60
AuNSH	Organosilica layer	-	50	808	MDA-MB-231 and MDA-MB-231 tumour bearing mice	≈ 55	Breast	Cell death induction of 90% in MDA-MB-231 and promotion of temperature increase to ≈58°C.	61

	PEG surface modified, SN38 modified	-	5	808	HCT 116 / HCT 116 tumour-bearing mice	≈ 53	Colorectal	Elevation of the tumour temperature to 53°C, leading to reduction of HCT116 cells growth.	[62]
	Surface modified with PEG, HSP70 and siRNA loaded	-	50	765	U87MG / U87MG tumour-bearing mice	≈ 48	Glioma	Elevation of tumour temperature to 46°C, leading to decrease the U87MG tumours' growth.	[63]
	Coated with liposomes containing betulinic acid	-	149.4	808	143B and HeLa /U14 tumour-bearing mice	T_{max} = 43	Osteosarcoma	Demonstrated highly efficient antitumour effects with an inhibition rate of 83.02%, thus presenting a crucial synergistic therapeutic effect of thermotherapy and chemotherapy	[64]
	Coated with Macrophage cell membrane camouflaged coated MS nanoparticles	-	12	808	4T1 cells / 4T1 tumour-bearing mice	ΔT = 30	Breast	Reserved the natural features of their source cells, which may enhance the efficacy of photothermal therapy and other noble-metal nanoparticles.	[65]
	siRNA	HER2	30	785	MFC	-	Gastric	Multiple platforms offering a promising translational treatment for gastric cancer.	[66]
	Aptamer modified	Aptamers	10-20 to 100-200	808	MRC-5, MCF-10A, A549, MCF-7	-	Lung	AuNPs selectively accumulated in tumour cells, this enhanced the reduction of tumour size and viability	[67]
AuNSP	Cisplatin loaded	-	50	808	MDA-MB-231	45	Breast	Enhance antitumour effect of breast cancer and DNA destruction by improving hypoxia in tumours	[68]

	CP-TPP/Au/PEG	-	196 ± 20	808	HeLa cells and human umbilical vein endothelial cells (HUVECs)	-	Cervical	The platform offers notable effectiveness to achieve PDT and PTT combination for enhanced cancer therapeutics.	69
	Ce6, Hyaluronidase Doxorubicin loaded	-	55	650	H22	-	Hepatocarcinoma	Presented significant advantages of multi-modal synergistic effects for cancer therapy by remotely controlling laser stimulus	70
AuNST	Gd chelates coated with Organosilica, PEG loaded	-	60	808	MDA-MB-231 and MDA-MB-231 tumour bearing mice	T_{max} = 68	Breast	Multifunctional AuNST is of excellent potential as a multifunctional nanoplatform for focused photothermal tumour therapy.	71
	Coated with FA	-	50	808	HeLa and A549 cells / HeLa tumour bearing mice	T_{max} = 51.27	Cervical	The exploration presented great potential in the early diagnosis and treatment of cancer.	72
	Coated with Bacteria-like mesoporous silica	-	30	980	Mouse sarcoma tumour-bearing mice	T_{max} = 42	Sarcoma	This exploration has the potential to be utilised for preoperative CT imaging, intraoperative detection, as well as image-guided photothermal therapy and in vivo biosensing	73
	-	-	141	808 and 635	4T1	ΔT = 17	Breast	Complete destruction of 4T1 tumour	74

	Hyaluronidase and TPP	CD44 and mitochondrion	-	808	SCC-7, MCF-7/ADR	ΔT > 20	Breast	Presented clear non-resistant or resistant tumour inhibition both in vitro and in vivo	75
	Coated with polydopamine stabilised with PEI	-	74.2	808	HeLa cells / HeLa tumour bearing mice	ΔT = 15.1	Cervical	The produced model may be used as a versatile platform for PTT of different types of cancers and targeted CT imaging	76
	Coated with RGD-modified dendrimer	-	55.1	808	U87MG / U87MG tumour-bearing mice	ΔT = 55	Glioblastoma	The developed multifunctional nanoplatform is promising for tumour imaging and combinational PTT and gene therapy.	77
	Coated with hollow MS encapsulated with PFH, PEG loaded	-	60	808	C6 / C6 tumour bearing mice	ΔT = 40.2	Glioma	The developed AuNPs may be used as a novel multifunctional theranostic nanoplatform for tumour multimode imaging and PTT.	78
	Surface modified with PEG and TAT peptide	-	D: 86	808	B16-F10 / B16-F10 tumour bearing mice	ΔT ≈ 40	Melanoma	Prevented tumour growth for 7 days followed by a slight increase in tumour volume until day 14.	79
	-	-	D: 27	808	PC3 / PC3 tumour bearing mice	ΔT ≈ 20	Prostate	The tumours' irradiation exhibited an 8, 14, and 10 °C increase in the tumour cells treated with the 27, 86, and 151 nm AuNSHs.	80
	Surface modified with PEG	-	D: 60	808	MCF-7 and MCF-7 tumour bearing mice	-	Adenocarcinoma	The platform exhibited a 20°C increase of the tumour' temperature that resulted in the decrease of the MCF-7 tumours' volume for 15 days.	81

	-	-	255	808	MDA-MB-231	17	Breast	Stable photothermal conversion with 40.5% efficiency and significant tranostatic efficiency	[82]
	Cisplatin loaded	-	≈ 65	808	MCF-7	80	Breast	Increased tumour damage through ferroptosis and ablation of localized tumours through efficient photothermal heating	[83]
	-	Peptides	80	-	A549, female BALB/c-nude mice	-	Lung	Exhibited significant stability and biocompatibility and presented effective internalisation by A549 cancer cells while exhibiting superior antitumour efficacy	[84]
	-	Peptides	82.5 ± 6.5	808	PC-3, DU145, LNCaP, 3T3 / nude mice	-	Prostate	Significant light-thermal conversion efficiency, biocompatibility, and strong cellular penetration.	[85]
AuNU	Doxorubicin loaded	Hyaluronidase	20	808	MDA-MB-231	40.2	Breast	Effective destruction of MDA-MB-231 cells without side effects	[86]

Supplementary Table 1B – Abbreviations list and their description

Abbreviation	Description
1321N1	Cell line of human astrocytoma
143B	Cell lines that are thymidine kinase deficient (TK-) and resistant to BUdR. 143B and HOS
293T cells	Cell lines of highly transfectable derivative of human embryonic kidney.
3T3	Several cell lines of mouse embryonic fibroblasts.
4T1	Cell line posing 6-thioguanine resistance
A375	Cell line exhibiting epithelial morphology that was isolated from the skin of a 54-year-old, female patient with malignant melanoma
A431	Cell line of human epidermoid carcinoma
A549	Cell line of lung carcinoma epithelial cells
AMH	Anti-Mullerian hormone
AS1411	Guanosine-rich oligonucleotide
AuNC	Gold Nanocages
AuNCL	Gold Nanoclusters
AuND	Gold Nanodumbless
AuNF	Gold Nanoflower
AuNM	Gold Nanomaterials
AuNP	Gold Nanoparticles
AuNPR	Gold Nanoprisims

AuNPY	Gold Nanopyrmids
AuNR	Gold Nanorods
AuNSH	Gold Nanoshells
AuNSP	Gold Nanospheres
AuNST	Gold Nanostars
AuNU	Gold Nanourchins
B16-F10	Cell line of murine melanoma
B16-F10 cells	Cell line exhibiting a morphology of spindle-shaped and epithelial-like cells that was isolated from skin tissue of a mouse with melanoma.
BSA	Bovine serum albumin
C57BL/6	Inbred strain of laboratory mouse
C6 glioma	Glial cell line that was isolated from the brain of a rat with Glioma
CD133	Prominin-1
CD33	Transmembrane receptor
CD44	Cell-surface glycoprotein antigen
CD56	Neural cell adhesion molecule
CD8	Transmembrane glycoprotein
CD8	Transmembrane glycoprotein
CDR	Chemo drug release
CDT	Chemodynamic therapy
Ce6	Chlorin e6

CIK-cells	Cytokine-induced killer cells
COS7	African green monkey kidney fibroblast-like cell line
CP-TTP	poly(cyclotriphosphazene-co-tetraphenylporphyrin-co-sulfonyldiphenol) nanospheres
CpG	5'—C—phosphate—G—3', Cytosine and guanine separated by only one phosphate group
CT	Computerized Tomography
CT26	Cell line of undifferentiated colon carcinoma, N-nitroso-N-methylurethane-(NNMU)
CTSE	Cathepsin E
DCs	Antigen-presenting cells for activating native T cells
DU145	Cell line with epithelial morphology isolated from the brain of a 69-year-old, White, male with prostate cancer.
EGF	Epidermal growth factor
EGFR	Epidermal growth factor receptor
EpCam	Epithelial cellular adhesion molecule
FA	Folic Acid
FR	Folate receptor
GCC827	Epithelial cell isolated from the lung of a White, 39-year-old female having adenocarcinoma
GD-chelates	Gadolinium chelates
H22	Mouse hepatocellular carcinoma (HCC) cell line
HA	Hyaluronic acid
HCC-LM3	Lung metastatic lesions of BALB/c nude mice bearing human hepatocellular carcinoma (HCC)
HCT 166	Cell line of human colorectal carcinoma
HeLa	HeLa Cell line

Hep G2	Cell line exhibiting epithelial-like morphology
HER2	Human epidermal growth factor receptor 2
HMSC	Normal Human Bone Marrow Derived Mesenchymal Stem Cells
HOB	Primary Human Osteoblasts isolated from femoral trabecular bone tissue
HOC313	Human oral squamous-cell-carcinoma cell line
HSC-3	Human oral squamous carcinoma cell line
HSP	Heat shock proteins
HSP70	Family of conserved ubiquitously expressed heat shock proteins.
HUVEC	Primary cells isolated from the vein of the umbilical cord
ICD	Immunogenic cell death
ICG	Indocyanine green
KB Cells	Human epithelial carcinoma cells
L02	Human foetal hepatocyte line
L929	Cell strains to be established in continuous culture
Lewis cells	Cell line established from the lung of a C57BL mouse bearing a tumour resulting from an implantation of primary Lewis lung carcinoma.
LF	Lactoferrin
LNCaP	Androgen-sensitive human prostate adenocarcinoma cells derived from the left supraclavicular lymph node metastasis from a 50-year-old caucasian male.
MCF-10A	Epithelial cell line
MCF-10A	Epithelial cell line isolated from the mammary gland of a White, 36-year-old female with fibrocystic breasts
MCF-7	Human breast cancer cell line

MCF-7/ADR	Adriamycin-resistant cell line, a multidrug-resistant breast cancer cell model
MDA-MB-231	Triple-negative breast cancer (TNBC) cell line
MDA-MB-468	Cell line, isolated from a pleural effusion of a 51-year-old Black female patient with metastatic adenocarcinoma of the breast.
MFC	Mouse gastric cancer cell line
MicroRNA-181b	MIR181B2 RNA Gene
MRC-5	Diploid cell culture line composed of fibroblasts
MRI	Magnetic resonance imaging
MS	Mesoporous Silica
N2a cells	Mouse neuroblasts with neuronal and amoeboid stem cell morphology isolated from brain tissue
NIH3T3	Cell line derived from mouse embryonic fibroblasts
p(NIPAM-co-AM)	Poly(N-isopropylacrylamide)
PAI	Photoacoustic imaging
PANC1	Cell line isolated from pancreatic duct of a patient with epithelioid carcinoma.
PC-3	Prostate cancer cell line
PDT	Photodynamic therapy
PEG	Polyethylene glycol
PEI	Polyethylenimine
PFH	Perflurohexane
PLGA	Polylactic-co-glycolic acid
PTT	Photothermal Therapy

R837	Imiquimod
RGD	Arginine-glycine-aspartic acid
SA	Serum Albumin
SCC7	Mouse head and neck carcinoma cell line
SCC8 tumour	An androgen-dependent tumour obtained by inoculating an androgen-responsive cell line
Si	Silica
siRNA	Silencing RNA
SKBR3	human breast cancer cell line
SMMC-7721	Human hepatocarcinoma cell line
SN38	(4S)-4,11-Diethyl-4,9-dihydroxy-1,4-dihydro-3H,14H-pyrano[3′,4′:6,7]indolizino[1,2-b]quinoline-3,14-dione
SW480	Cells isolated from the large intestine of a Dukes C colorectal cancer patient
TAT PEPTIDE	Transactivator of transcription (TAT) of human immunodeficiency virus and is a Cell-penetrating peptides.
U14	Cervical tumour cell lines
U373-MG	human glioblastoma cell line
U87MG	human glioblastoma cell line

References

1. Xu X, Chong Y, Liu X, et al. Multifunctional nanotheranostic gold nanocages for photoacoustic imaging guided radio/photodynamic/photothermal synergistic therapy. *Acta Biomaterialia*. 2019/01/15/ 2019;84:328-338. doi:https://doi.org/10.1016/j.actbio.2018.11.043

2. Zhu DM, Xie W, Xiao YS, et al. Erythrocyte membrane-coated gold nanocages for targeted photothermal and chemical cancer therapy. *Nanotechnology*. Feb 23 2018;29(8):084002. doi:10.1088/1361-6528/aa9ca1

3. Wang Z, Chen Z, Liu Z, et al. A multi-stimuli responsive gold nanocage-hyaluronic platform for targeted photothermal and chemotherapy. *Biomaterials*. Dec 2014;35(36):9678-88. doi:10.1016/j.biomaterials.2014.08.013

4. Feng Y, Cheng Y, Chang Y, et al. Time-staggered delivery of erlotinib and doxorubicin by gold nanocages with two smart polymers for reprogrammable release and synergistic with photothermal therapy. *Biomaterials*. Oct 2019;217:119327. doi:10.1016/j.biomaterials.2019.119327

5. Huang S, Duan S, Wang J, et al. Folic-Acid-Mediated Functionalized Gold Nanocages for Targeted Delivery of Anti-miR-181b in Combination of Gene Therapy and Photothermal Therapy against Hepatocellular Carcinoma. *Advanced Functional Materials*. 2016;26(15):2532-2544. doi:https://doi.org/10.1002/adfm.201504912

6. Chang Y, Feng Y, Cheng Y, et al. Anisotropic Plasmonic Metal Heterostructures as Theranostic Nanosystems for Near Infrared Light-Activated Fluorescence Amplification and Phototherapy. *Advanced Science*. 2019;6(11):1900158. doi:https://doi.org/10.1002/advs.201900158

7. Sun H, Su J, Meng Q, et al. Cancer Cell Membrane-Coated Gold Nanocages with Hyperthermia-Triggered Drug Release and Homotypic Target Inhibit Growth and Metastasis of Breast Cancer. *Advanced Functional Materials*. 2017;27(3):1604300. doi:https://doi.org/10.1002/adfm.201604300

8. Jenkins SV, Nedosekin DA, Miller EK, et al. Galectin-1-based tumour-targeting for gold nanostructure-mediated photothermal therapy. *Int J Hyperthermia*. Feb 2018;34(1):19-29. doi:10.1080/02656736.2017.1317845

9. Yu Y, Zhang Z, Wang Y, et al. A new NIR-triggered doxorubicin and photosensitizer indocyanine green co-delivery system for enhanced multidrug resistant cancer treatment through simultaneous chemo/photothermal/photodynamic therapy. *Acta Biomater*. Sep 1 2017;59:170-180. doi:10.1016/j.actbio.2017.06.026

10. Han HS, Choi KY, Lee H, et al. Gold-Nanoclustered Hyaluronan Nano-Assemblies for Photothermally Maneuvered Photodynamic Tumor Ablation. *ACS Nano*. 2016/12// 2016;10(12):10858-10868. doi:10.1021/acsnano.6b05113

11. Zhao P, Liu S, Wang L, et al. Alginate mediated functional aggregation of gold nanoclusters for systemic photothermal therapy and efficient renal clearance. *Carbohydr Polym*. Aug 1 2020;241:116344. doi:10.1016/j.carbpol.2020.116344

12. Park S, Kim H, Lim SC, et al. Gold nanocluster-loaded hybrid albumin nanoparticles with fluorescence-based optical visualization and photothermal conversion for tumor detection/ablation. *J Control Release*. Jun 28 2019;304:7-18. doi:10.1016/j.jconrel.2019.04.036

13. Higbee-Dempsey E, Amirshaghaghi A, Case MJ, Miller J, Busch TM, Tsourkas A. Indocyanine Green–Coated Gold Nanoclusters for Photoacoustic Imaging and Photothermal Therapy. *Advanced Therapeutics*. 2019;2(9):1900088. doi:https://doi.org/10.1002/adtp.201900088

14. Liu R, Hu C, Yang Y, Zhang J, Gao H. Theranostic nanoparticles with tumor-specific enzyme-triggered size reduction and drug release to perform photothermal therapy for breast cancer treatment. *Acta Pharmaceutica Sinica B*. 2019/03/01/ 2019;9(2):410-420. doi:https://doi.org/10.1016/j.apsb.2018.09.001

15. Li H, Wang P, Deng Y, et al. Combination of active targeting, enzyme-triggered release and fluorescent dye into gold nanoclusters for endomicroscopy-guided photothermal/photodynamic therapy to pancreatic ductal adenocarcinoma. *Biomaterials*. Sep 2017;139:30-38. doi:10.1016/j.biomaterials.2017.05.030

16. Xing Y, Kang T, Luo X, Zhu J, Wu P, Cai C. Coral-shaped Au nanostructures for selective apoptosis induction during photothermal therapy. 10.1039/C9TB01503E. *Journal of Materials Chemistry B*. 2019;7(40):6224-6231. doi:10.1039/C9TB01503E

17. Zhang Y, Song T, Feng T, et al. Plasmonic modulation of gold nanotheranostics for targeted NIR-II photothermal-augmented immunotherapy. *Nano Today*. 2020/12/01/ 2020;35:100987. doi:https://doi.org/10.1016/j.nantod.2020.100987

18. Liu J, Zhai F, Zhou H, Yang W, Zhang S. Nanogold Flower-Inspired Nanoarchitectonics Enables Enhanced Light-to-Heat Conversion Ability for Rapid and Targeted Chemo-Photothermal Therapy of a Tumor. *Adv Healthc Mater*. Apr 2019;8(8):e1801300. doi:10.1002/adhm.201801300

19. Wang H, An L, Tao C, et al. A smart theranostic platform for photoacoustic and magnetic resonance dual-imaging-guided photothermal-enhanced chemodynamic therapy. 10.1039/C9NR10039C. *Nanoscale*. 2020;12(8):5139-5150. doi:10.1039/C9NR10039C

20. Wang M, Chang M, Chen Q, et al. Au(2)Pt-PEG-Ce6 nanoformulation with dual nanozyme activities for synergistic chemodynamic therapy / phototherapy. *Biomaterials*. Sep 2020;252:120093. doi:10.1016/j.biomaterials.2020.120093

21. Fan L, Xu X, Zhu C, et al. Tumor Catalytic–Photothermal Therapy with Yolk–Shell Gold@Carbon Nanozymes. *ACS Applied Materials & Interfaces*. 2018/02/07 2018;10(5):4502-4511. doi:10.1021/acsami.7b17916

22. Wang Z, Ju Y, Tong S, et al. Au3Cu tetrapod nanocrystals: highly efficient and metabolizable multimodality imaging-guided NIR-II photothermal agents. 10.1039/C8NH00135A. *Nanoscale Horizons*. 2018;3(6):624-631. doi:10.1039/C8NH00135A

23. Gao F, He G, Yin H, et al. Titania-coated 2D gold nanoplates as nanoagents for synergistic photothermal/sonodynamic therapy in the second near-infrared window. 10.1039/C8NR07188H. *Nanoscale*. 2019;11(5):2374-2384. doi:10.1039/C8NR07188H

24. Kim HS, Lee SJ, Lee DY. Milk protein-shelled gold nanoparticles with gastrointestinally active absorption for aurotherapy to brain tumor. *Bioact Mater*. Feb 2022;8:35-48. doi:10.1016/j.bioactmat.2021.06.026

25. Keyvan Rad J, Mahdavian AR, Khoei S, Shirvalilou S. Enhanced Photogeneration of Reactive Oxygen Species and Targeted Photothermal Therapy of C6 Glioma Brain Cancer Cells by Folate-Conjugated Gold–Photoactive Polymer Nanoparticles. *ACS Applied Materials & Interfaces*. 2018/06/13 2018;10(23):19483-19493. doi:10.1021/acsami.8b05252

26. Yu S, Zhou Y, Sun Y, et al. Endogenous mRNA Triggered DNA-Au Nanomachine for In Situ Imaging and Targeted Multimodal Synergistic Cancer Therapy. *Angew Chem Int Ed Engl*. Mar 8 2021;60(11):5948-5958. doi:10.1002/anie.202012801

27. Agabeigi R, Rasta SH, Rahmati-Yamchi M, Salehi R, Alizadeh E. Novel Chemo-Photothermal Therapy in Breast Cancer Using Methotrexate-Loaded Folic Acid Conjugated Au@SiO(2) Nanoparticles. *Nanoscale Res Lett*. Mar 19 2020;15(1):62. doi:10.1186/s11671-020-3295-1

28. Wei Q, He J, Wang S, et al. Low-dose X-ray enhanced tumor accumulation of theranostic nanoparticles for high-performance bimodal imaging-guided photothermal therapy. *Journal of Nanobiotechnology*. 2021/05/26 2021;19(1):155. doi:10.1186/s12951-021-00875-8

29. Cheng X, Zhou X, Xu J, et al. Furin Enzyme and pH Synergistically Triggered Aggregation of Gold Nanoparticles for Activated Photoacoustic Imaging and Photothermal Therapy of Tumors. *Anal Chem*. Jul 6 2021;93(26):9277-9285. doi:10.1021/acs.analchem.1c01713

30. Zhang Y, Zhou L, Tan J, Liu J, Shan X, Ma Y. Laser-triggered collaborative chemophotothermal effect of gold nanoparticles for targeted colon cancer therapy. *Biomed Pharmacother*. Oct 2020;130:110492. doi:10.1016/j.biopha.2020.110492

31. Buonerba A, Lapenta R, Donniacuo A, et al. NIR multiphoton ablation of cancer cells, fluorescence quenching and cellular uptake of dansyl-glutathione-coated gold nanoparticles. *Scientific Reports*. 2020/07/09 2020;10(1):11380. doi:10.1038/s41598-020-68397-1

32. Li B, Sun L, Li T, et al. Ultra-small gold nanoparticles self-assembled by gadolinium ions for enhanced photothermal/photodynamic liver cancer therapy. 10.1039/D0TB02410D. *Journal of Materials Chemistry B*. 2021;9(4):1138-1150. doi:10.1039/D0TB02410D

33. Mocan L, Matea C, Tabaran FA, et al. Photothermal treatment of liver cancer with albumin-conjugated gold nanoparticles initiates Golgi Apparatus-ER dysfunction and caspase-3 apoptotic pathway activation by selective targeting of Gp60 receptor. *Int J Nanomedicine*. 2015;10:5435-45. doi:10.2147/ijn.S86495

34. Ma Y, Chen L, Li X, et al. Rationally integrating peptide-induced targeting and multimodal therapies in a dual-shell theranostic platform for orthotopic metastatic spinal tumors. *Biomaterials*. Aug 2021;275:120917. doi:10.1016/j.biomaterials.2021.120917

35. Yata T, Takahashi Y, Tan M, et al. DNA nanotechnology-based composite-type gold nanoparticle-immunostimulatory DNA hydrogel for tumor photothermal immunotherapy. *Biomaterials*. Nov 2017;146:136-145. doi:10.1016/j.biomaterials.2017.09.014

36. Yang S, Yao D, Wang Y, Yang W, Zhang B, Wang D. Enzyme-triggered self-assembly of gold nanoparticles for enhanced retention effects and photothermal therapy of prostate cancer. 10.1039/C8CC05136D. *Chemical Communications*. 2018;54(70):9841-9844. doi:10.1039/C8CC05136D

37. Liu B, Qiao G, Han Y, et al. Targeted theranostics of lung cancer: PD-L1-guided delivery of gold nanoprisms with chlorin e6 for enhanced imaging and photothermal/photodynamic therapy. *Acta Biomater*. Nov 2020;117:361-373. doi:10.1016/j.actbio.2020.09.040

38. Zhao S, Tian Y, Liu W, et al. High and low molecular weight hyaluronic acid-coated gold nanobipyramids for photothermal therapy. 10.1039/C7RA11667E. *RSC Advances*. 2018;8(16):9023-9030. doi:10.1039/C7RA11667E

39. Feng J, Chen L, Xia Y, et al. Bioconjugation of Gold Nanobipyramids for SERS Detection and Targeted Photothermal Therapy in Breast Cancer. *ACS Biomaterials Science & Engineering*. 2017/04/10 2017;3(4):608-618. doi:10.1021/acsbiomaterials.7b00021

40. Wang Y, Li M, Luo T, et al. Development of FL/MR dual-modal Au nanobipyramids for targeted cancer imaging and photothermal therapy. *Mater Sci Eng C Mater Biol Appl*. Aug 2021;127:112190. doi:10.1016/j.msec.2021.112190

41. Song J, Yang X, Jacobson O, et al. Ultrasmall Gold Nanorod Vesicles with Enhanced Tumor Accumulation and Fast Excretion from the Body for Cancer Therapy. *Adv Mater*. Sep 2 2015;27(33):4910-7. doi:10.1002/adma.201502486

42. Zhu H, Chen Y, Yan F-J, et al. Polysarcosine brush stabilized gold nanorods for in vivo near-infrared photothermal tumor therapy. *Acta Biomaterialia*. 12/01 2016;50doi:10.1016/j.actbio.2016.12.050

43. Wang X, Gao S, Qin Z, et al. Evans Blue Derivative-Functionalized Gold Nanorods for Photothermal Therapy-Enhanced Tumor Chemotherapy. *ACS Applied Materials & Interfaces*. 2018/05/02 2018;10(17):15140-15149. doi:10.1021/acsami.8b02195

44. Lee C, Hwang HS, Lee S, et al. Rabies Virus-Inspired Silica-Coated Gold Nanorods as a Photothermal Therapeutic Platform for Treating Brain Tumors. *Adv Mater*. Apr 2017;29(13)doi:10.1002/adma.201605563

45. Xu C, Chen F, Valdovinos HF, et al. Bacteria-like mesoporous silica-coated gold nanorods for positron emission tomography and photoacoustic imaging-guided chemo-photothermal combined therapy. *Biomaterials*. May 2018;165:56-65. doi:10.1016/j.biomaterials.2018.02.043

46. Luo G-F, Chen W-H, Lei Q, et al. A Triple-Collaborative Strategy for High-Performance Tumor Therapy by Multifunctional Mesoporous Silica-Coated Gold Nanorods. *Advanced Functional Materials*. 2016;26(24):4339-4350. doi:https://doi.org/10.1002/adfm.201505175

47. Liu X, Huang N, Li H, Wang H, Jin Q, Ji J. Multidentate Polyethylene Glycol Modified Gold Nanorods for in Vivo Near-Infrared Photothermal Cancer Therapy. *ACS Applied Materials & Interfaces*. 2014/04/23 2014;6(8):5657-5668. doi:10.1021/am5001823

48. Liu J, Liang H, Li M, et al. Tumor acidity activating multifunctional nanoplatform for NIR-mediated multiple enhanced photodynamic and photothermal tumor therapy. *Biomaterials*. Mar 2018;157:107-124. doi:10.1016/j.biomaterials.2017.12.003

49. Li Y, Duy Le TM, Nam Bui Q, Yang HY, Lee DS. Tumor acidity and CD44 dual targeting hyaluronic acid-coated gold nanorods for combined chemo- and photothermal cancer therapy. *Carbohydr Polym*. Dec 15 2019;226:115281. doi:10.1016/j.carbpol.2019.115281

50. Xu W, Qian J, Hou G, et al. Hyaluronic Acid-Functionalized Gold Nanorods with pH/NIR Dual-Responsive Drug Release for Synergetic Targeted Photothermal Chemotherapy of Breast Cancer. *ACS Applied Materials & Interfaces*. 2017/10/25 2017;9(42):36533-36547. doi:10.1021/acsami.7b08700

51. Li Y, He L, Dong H, et al. Fever-Inspired Immunotherapy Based on Photothermal CpG Nanotherapeutics: The Critical Role of Mild Heat in Regulating Tumor Microenvironment. *Advanced Science*. 2018;5(6):1700805. doi:https://doi.org/10.1002/advs.201700805

52. Chen J, Lin L, Yan N, et al. Macrophages loaded CpG and GNR-PEI for combination of tumor photothermal therapy and immunotherapy. *SCIENCE CHINA Materials*. 2018;61(2095-8226):1484. doi:https://doi.org/10.1007/s40843-018-9238-6

53. Zhang D, Ye Z, Liu H, et al. Cell membrane coated smart two-dimensional supraparticle for in vivo homotypic cancer targeting and enhanced combinational theranostics. Research Paper. *Nanotheranostics*. 2021;5(3):275-287. doi:10.7150/ntno.57657

54. Xu C, Zhang T, Lu G, et al. Disulfiram-gold-nanorod integrate for effective tumor targeting and photothermal-chemical synergistic therapy. 10.1039/D0BM00062K. *Biomaterials Science*. 2020;8(12):3310-3319. doi:10.1039/D0BM00062K

55. Chuang CC, Cheng CC, Chen PY, et al. Gold nanorod-encapsulated biodegradable polymeric matrix for combined photothermal and chemo-cancer therapy. *Int J Nanomedicine*. 2019;14:181-193. doi:10.2147/ijn.S177851

56. Tao Y, Ju E, Liu Z, Dong K, Ren J, Qu X. Engineered, self-assembled near-infrared photothermal agents for combined tumor immunotherapy and chemo-photothermal therapy. *Biomaterials*. Aug 2014;35(24):6646-56. doi:10.1016/j.biomaterials.2014.04.073

57. Yang H, He H, Tong Z, Xia H, Mao Z, Gao C. The impact of size and surface ligand of gold nanorods on liver cancer accumulation and photothermal therapy in the second near-infrared window. *J Colloid Interface Sci*. Apr 1 2020;565:186-196. doi:10.1016/j.jcis.2020.01.026

58. Ye B, Zhao B, Wang K, et al. Neutrophils mediated multistage nanoparticle delivery for prompting tumor photothermal therapy. *Journal of Nanobiotechnology*. 2020/09/29 2020;18(1):138. doi:10.1186/s12951-020-00682-7

59. Li Z, Huang P, Zhang X, et al. RGD-Conjugated Dendrimer-Modified Gold Nanorods for in Vivo Tumor Targeting and Photothermal Therapy. *Molecular Pharmaceutics*. 2010/02/01 2010;7(1):94-104. doi:10.1021/mp9001415

60. Xu H, Sheng G, Lu L, et al. GRPr-mediated photothermal and thermodynamic dual-therapy for prostate cancer with synergistic anti-apoptosis mechanism. 10.1039/D0NR07196J. *Nanoscale*. 2021;13(7):4249-4261. doi:10.1039/D0NR07196J

61. Gao Y, Li Y, Wang Y, et al. Multilayered Nanoshells: Controlled Synthesis of Multilayered Gold Nanoshells for Enhanced Photothermal Therapy and SERS Detection (Small 1/2015). *Small*. 2015;11(1):144-144. doi:https://doi.org/10.1002/smll.201570007

62. Lee S-Y, Peng C-L, Shieh M-J. Combined Chemo-Photothermotherapy Using Gold Nanoshells on Drug-Loaded Micellar Templates for Colorectal Cancer Treatment. *Particle & Particle Systems Characterization*. 2018;35(12):1800334. doi:https://doi.org/10.1002/ppsc.201800334

63. Wang Z, Li S, Zhang M, et al. Laser-Triggered Small Interfering RNA Releasing Gold Nanoshells against Heat Shock Protein for Sensitized Photothermal Therapy. *Advanced Science*. 2017;4(2):1600327. doi:https://doi.org/10.1002/advs.201600327

64. Liu Y, Zhang X, Liu Z, et al. Gold nanoshell-based betulinic acid liposomes for synergistic chemo-photothermal therapy. *Nanomedicine*. Aug 2017;13(6):1891-1900. doi:10.1016/j.nano.2017.03.012

65. Xuan M, Shao J, Dai L, Li J, He Q. Macrophage Cell Membrane Camouflaged Au Nanoshells for in Vivo Prolonged Circulation Life and Enhanced Cancer Photothermal Therapy. *ACS Applied Materials & Interfaces*. 2016/04/20 2016;8(15):9610-9618. doi:10.1021/acsami.6b00853

66. Zhang J, Zhao T, Han F, Hu Y, Li Y. Photothermal and gene therapy combined with immunotherapy to gastric cancer by the gold nanoshell-based system. *Journal of Nanobiotechnology*. 2019/07/05 2019;17(1):80. doi:10.1186/s12951-019-0515-x

67. Kalinowska D, Grabowska-Jadach I, Liwinska M, et al. Studies on effectiveness of PTT on 3D tumor model under microfluidic conditions using aptamer-modified nanoshells. *Biosens Bioelectron*. Feb 1 2019;126:214-221. doi:10.1016/j.bios.2018.10.069

68. Cui G, He P, Yu L, Wen C, Xie X, Yao G. Oxygen self-enriched nanoplatform combined with US imaging and chemo/photothermal therapy for breast cancer. *Nanomedicine*. Oct 2020;29:102238. doi:10.1016/j.nano.2020.102238

69. Wei X, Chen H, Tham HP, et al. Combined Photodynamic and Photothermal Therapy Using Cross-Linked Polyphosphazene Nanospheres Decorated with Gold Nanoparticles. *ACS Applied Nano Materials*. 2018/07/27 2018;1(7):3663-3672. doi:10.1021/acsanm.8b00776

70. Deng X, Chen Y, Cheng Z, et al. Rational design of a comprehensive cancer therapy platform using temperature-sensitive polymer grafted hollow gold nanospheres: simultaneous chemo/photothermal/photodynamic therapy triggered by a 650 nm laser with enhanced anti-tumor efficacy. 10.1039/C5NR08253F. *Nanoscale*. 2016;8(12):6837-6850. doi:10.1039/C5NR08253F

71. Gao Y, Li Y, Chen J, et al. Multifunctional gold nanostar-based nanocomposite: Synthesis and application for noninvasive MR-SERS imaging-guided photothermal ablation. *Biomaterials*. 2015/08/01/ 2015;60:31-41. doi:https://doi.org/10.1016/j.biomaterials.2015.05.004

72. An J, Yang XQ, Cheng K, et al. In Vivo Computed Tomography/Photoacoustic Imaging and NIR-Triggered Chemo-Photothermal Combined Therapy Based on a Gold Nanostar-, Mesoporous Silica-, and Thermosensitive Liposome-Composited Nanoprobe. *ACS Appl Mater Interfaces*. Dec 6 2017;9(48):41748-41759. doi:10.1021/acsami.7b15296

73. Liu Y, Ashton JR, Moding EJ, et al. A Plasmonic Gold Nanostar Theranostic Probe for In Vivo Tumor Imaging and Photothermal Therapy. *Theranostics*. 2015;5(9):946-60. doi:10.7150/thno.11974

74. Li Z, Yang F, Wu D, et al. Ce6-Conjugated and polydopamine-coated gold nanostars with enhanced photoacoustic imaging and photothermal/photodynamic therapy to inhibit lung metastasis of breast cancer. 10.1039/D0NR05386D. *Nanoscale*. 2020;12(43):22173-22184. doi:10.1039/D0NR05386D

75. Chen S, Lei Q, Qiu WX, et al. Mitochondria-targeting "Nanoheater" for enhanced photothermal/chemo-therapy. *Biomaterials*. Feb 2017;117:92-104. doi:10.1016/j.biomaterials.2016.11.056

76. Li D, Zhang Y, Wen S, et al. Construction of polydopamine-coated gold nanostars for CT imaging and enhanced photothermal therapy of tumors: an innovative theranostic strategy. 10.1039/C6TB00773B. *Journal of Materials Chemistry B*. 2016;4(23):4216-4226. doi:10.1039/C6TB00773B

77. Wei P, Chen J, Hu Y, et al. Dendrimer-Stabilized Gold Nanostars as a Multifunctional Theranostic Nanoplatform for CT Imaging, Photothermal Therapy, and Gene Silencing of Tumors. *Adv Healthc Mater*. Dec 2016;5(24):3203-3213. doi:10.1002/adhm.201600923

78. Li X, Xing L, Zheng K, et al. Formation of Gold Nanostar-Coated Hollow Mesoporous Silica for Tumor Multimodality Imaging and Photothermal Therapy. *ACS Applied Materials & Interfaces*. 2017/02/22 2017;9(7):5817-5827. doi:10.1021/acsami.6b15185

79. Xu P, Ning P, Wang J, Qin Y, Liang F, Cheng Y. Precise control of apoptosis via gold nanostars for dose dependent photothermal therapy of melanoma. 10.1039/C9TB01956A. *Journal of Materials Chemistry B*. 2019;7(44):6934-6944. doi:10.1039/C9TB01956A

80. Espinosa A, Silva AK, Sánchez-Iglesias A, et al. Cancer Cell Internalization of Gold Nanostars Impacts Their Photothermal Efficiency In Vitro and In Vivo: Toward a Plasmonic Thermal Fingerprint in Tumoral Environment. *Adv Healthc Mater*. May 2016;5(9):1040-8. doi:10.1002/adhm.201501035

81. Tian Y, Luo S, Yan H, et al. Gold nanostars functionalized with amine-terminated PEG for X-ray/CT imaging and photothermal therapy. 10.1039/C5TB00509D. *Journal of Materials Chemistry B*. 2015;3(21):4330-4337. doi:10.1039/C5TB00509D

82. Zhang L, Liu C, Gao Y, et al. ZD2-Engineered Gold Nanostar@Metal-Organic Framework Nanoprobes for T(1) -Weighted Magnetic Resonance Imaging and Photothermal Therapy Specifically Toward Triple-Negative Breast Cancer. *Adv Healthc Mater*. Dec 2018;7(24):e1801144. doi:10.1002/adhm.201801144

83. del Valle AC, Yeh C-K, Huang Y-F. Near Infrared-Activatable Platinum-Decorated Gold Nanostars for Synergistic Photothermal/Ferroptotic Therapy in Combating Cancer Drug Resistance. *Advanced Healthcare Materials*. 2020;9(20):2000864. doi:https://doi.org/10.1002/adhm.202000864

84. Xia F, Niu J, Hong Y, et al. Matrix metallopeptidase 2 targeted delivery of gold nanostars decorated with IR-780 iodide for dual-modal imaging and enhanced photothermal/photodynamic therapy. *Acta Biomater*. Apr 15 2019;89:289-299. doi:10.1016/j.actbio.2019.03.008

85. Huang L, Xu C, Xu P, et al. Intelligent Photosensitive Mesenchymal Stem Cells and Cell-Derived Microvesicles for Photothermal Therapy of Prostate Cancer. *Nanotheranostics*. 2019;3(1):41-53. doi:10.7150/ntno.28450

86. Zhang B, Wang J, Sun J, et al. Self-Reporting Gold Nanourchins for Tumor-Targeted Chemo-Photothermal Therapy Integrated with Multimodal Imaging. *Advanced Therapeutics*. 2020;3(10):2000114. doi:https://doi.org/10.1002/adtp.202000114